Acta of Bioengineering and Biomechanics
Vol. 14, No. 4, 2012

Original paper
DOI: 10.5277/abb120410

Stochastic impulsive pressure calculations for time dependent human hip joint lubrication

KRZYSZTOF WIERZCHOLSKI*

Institute of Mechatronics, Nanotechnology and Vacuum Technique, Technical University of Koszalin, Poland.

The present paper is concerned with the calculation of the stochastic unsteady, impulsive pressure distributions and load carrying capacities in human hip joint for unsteady stochastic conditions, various standard deviations and Gaussian probability density function. The total changes of hydrodynamic pressure caused by viscoelastic synovial fluid properties are completely estimated. Calculations are performed in a super thin layer of biological synovial fluid inside the slide hip joint gap limited by a spherical bone head. Using a new unified operator of summation (UOS) method, the numerical topology of pressure calculation for a difference method is applied. From numerical standpoint the proposed method of solving modified hydrodynamic equations reduces this problem to resolving the partial recurrence non-homogeneous equation of second order with variable coefficients.

Key words: *stochastic, impulsive, pressure, load carrying capacity, unified numerical algorithm*

1. Introduction

The problem of hip joint lubrication after injury for unsteady impulsive motion has already been considered in KNOLL's papers [9], [25], in the monographs of Dowson [2], Mow et al. [10] and CWANEK [1], as well as in the author's papers [23], [24]. In the above publications, the computational model had not been accommodated to the spherical coordinates and had not been coupled with the unified calculation algorithm [18]. Contrary to the previous papers [23], [24] the present paper utilizes a new unified calculation algorithm for stochastic impulsive load carrying capacity determination of intelligent lubrication of spherical, biobearing human hip joint surfaces. Such algorithm satisfies stability conditions of numerical solutions of partial differential equations and gives real values of fluid velocity components and carrying capacities occurring in human hip joints. The above problems are the continuation of scientific research illustrated in the author's papers [14]–[24].

A rough and used cartilage surface in human hip joint suddenly changes its lubrication parameters after injury. Stochastic changes of roughness of bone head surfaces, and stochastic changes of the load imply random changes of gap height. Hence, pressure distributions and load carrying capacities radically decrease or increase their values in several microseconds after the trauma. These changes are very difficult to measure, hence to perform an appropriate numerical research in this field is very important. To obtain the right numerical results we must perform calculations using stochastic description with optimum standard deviations.

New values of capacities of human hip joint which occur during some microseconds after injury, very often decide on further development of disease or damage of the joint, caused by the trauma. Therefore the knowledge of lubrication parameters on the grounds of random conditions, for example, changes

* Corresponding author: Krzysztof Wierzcholski, Technical University of Koszalin, Institute of Mechatronics, Nanotechnology and Vacuum Technique, ul. Śniadeckich 2, 75-453 Koszalin, Poland. Tel.: +48 94 3478344, fax: +48 94 3426753, e-mail: krzysztof.wierzcholski@wp.pl

Received: July 7th, 2011
Accepted for publication: August 3rd, 2012

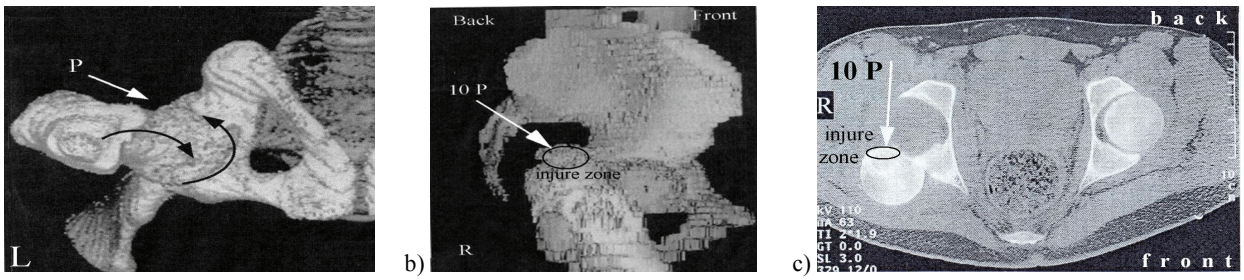

Fig. 1. X-ray imaging of early and final changes of gap height after injury: (a) negligibly small gap height changes caused by the force P in human left hip joint, (b) dislocation of bone head of right hip joint caused by the force $10 \times P$, (c) imaging of final changes

in some microseconds after trauma, is necessary for further diagnoses and therapy. The concentrated force P applied onto the external surface zone of tissue, causes an injury and dislocation of human hip joint.

If the concentrated force P is not large, the deformations of human body and deformations of joint cartilage surface generate only small changes in gap height of human hip joint (see the bone head shown in figure 1a). If the concentrated force is sufficiently large, e.g., it amounts to 10 P, then we can observe a dislocation of the bone head and acetabulum of human hip joint (see the bone head shown in figure 1b, 1c). The problem of lubrication of human hip joint after injury for random conditions has not been presented in papers mentioned in references [1]–[13].

1.1. The aim of research

- To show the hydrodynamic pressure determination in human hip joint under stochastic, unsteady and impulsive condition with symmetric probability density function.
- To indicate the time dependent pressure and load carrying capacity changes caused by the impulsive lubrication for various standard deviation.
- To illustrate the semi-numerical and analytical method of stochastic impulsive pressure calculation implemented by the Mathcad 12 Professional Program, and by convergent recurrence solutions of partial difference and differential equations with variable coefficients occurring in hydrodynamic lubrication theory.

2. Materials and methods

Description of real gap height changes depends on the variations of cartilage surface. Random changes of cartilage surface are described by the probability density functions on the basis of comparison between the results of CWANEK and WIERZCHOLSKI'S experiments [20]–[22] and the investigations of DOWSON and MOW [1], [10], see figure 2a, 2b. The measurements of values of changes on the sample surface (10 mm × 10 mm) of a pathological cartilage resting on the sphere, see figure 2a, 2b, of bone head of human hip joint have been performed by using the micro-sensor laser installed in the Rank–Taylor–Hobson–Talyscan–150 Apparatus, and elaborated by means of the Talymap Expert and Microsoft Excel Computer Program.

From 29 surgical measured samples the following parameters have been calculated: *St*, *Sz*, *Sa* of surface roughness expressed in micrometers. We calculate, for example: *St* – differences between values of rises and deeps of bone head surfaces in human hip joint, *Sz* – arithmetic mean between values of 5 rises and 5 deeps of bone head surface, *Sa* – standard deviation of probability density function of roughness distribution of cartilage surface [21], [22].

The measured values of *St* oscillate within the interval from 9.79 to 24.7 micrometers. The measured *Sz* values fluctuate within the interval from 8.52 to 14.7 micrometers. Finally, we find that the calculated values of *Sa* are contained in the interval from 0.78 to 1.96 micrometer. The symmetric Gaussian probability density function has been prepared by virtue of the above measured values. Proper description of random part of gap height changes depends on the appropriate selection of probability density function. As a criterion of estimation we choose the standard deviation. The probability density functions refer to the changes of cartilage surface, i.e., changes of gap height caused by the vibrations and roughness, respectively. From the measurements performed it follows that the height of roughness on the cartilage surface attains values from 0.05 to 0.25 mm.

The dimensionless gap height ε_{T1} depends on the spherical coordinates φ, ϑ_1 in circumferential, meridian directions and dimensionless time t_1, thus consists of two parts [20]:

$$\varepsilon_{T1} = \varepsilon_{T1s}(\varphi, \vartheta_1, t_1) + \delta_1(\varphi, \vartheta_1, \xi), \tag{1}$$

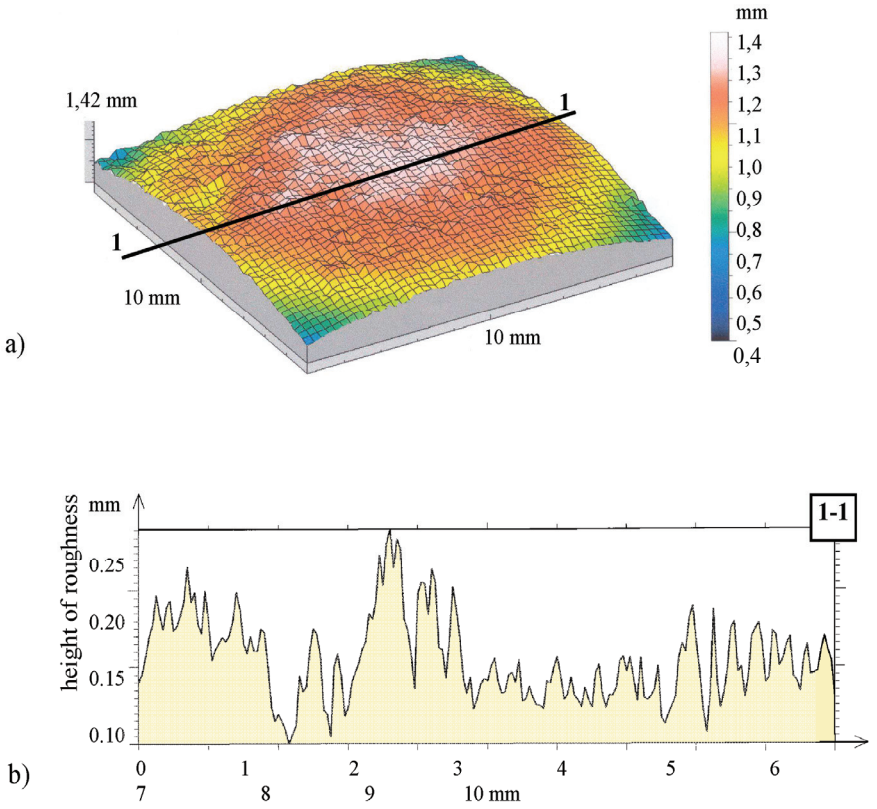

Fig. 2. Random changes of joint gap height due to the vibration and unsteady load: a) measurement of roughness values on the sample surface (10 mm × 10 mm) of used and pathological cartilage taken from the bone head of the human hip joint, b) longitudinal section of flatted surface of used joint cartilage of bone head with the asperity height of 1.4 mm measured by the laser sensor

where ε_{T1s} denotes the total dimensionless height of nominally smooth part of the thin fluid layer. This part of gap height contains dimensionless corrections of gap height caused by the hyper elastic cartilage deformations. The symbol δ_1 denotes the dimensionless random part of changes of gap height resulting from the vibrations, unsteady loading and surface roughness asperities of cartilage measured from the nominal mean level.

The symbol ξ describes the random variable, which characterizes the vibration unsteady load and roughness arrangement. Expectancy operator is defined by [3], [20], [22]:

$$E(*) = \int_{-\infty}^{+\infty} (*) \times f(\delta_1) d\delta_1, \tag{2}$$

$$f(\delta_1) \equiv \begin{cases} \left(1 - \dfrac{\delta_1^2}{c_1^2}\right)^5 & \text{for } -c_1 \le \delta_1 \le +c_1 \\ 0 & \text{for } |\delta_1| > c_1 \end{cases} \tag{3}$$

$$\sigma_{s1} = \frac{c_1}{\sqrt{13}} = 0.375,$$

where f describes a certain dimensionless Gaussian probability density function. Symbol $c_1 = 1.353515$ denotes the half total range of random variable of the thin layer thickness for normal hip joint (see [20], [22]). The symbol $\sigma_{s1} = 0.37539$ denotes the dimensionless standard deviation. To obtain dimensional value of the standard deviation σ_s we must multiply σ_{s1} by the characteristic value of gap height $\varepsilon_0 = 10 \cdot 10^{-6}$ m. In this case, the dimensional standard deviation equals 3.7 micrometers. From the measurements we have obtained the standard deviation value of about 3.5 micrometers for normal cartilage.

From the experiments performed it follows that the time-dependent gap height with perturbations and stochastic changes has the following dimensionless form [15], [20]:

$$\varepsilon_{T1} = \varepsilon_{T1s}(\varphi, \vartheta_1, t_1) + \delta_1$$

$$= \varepsilon_{T1s}(\varphi, \vartheta_1)\,[1 + s_1 \exp(-t_0 t_1 \omega_0)] + \delta_1. \tag{4}$$

After geometrical derivations there follows that the time-independent value of the smooth part of the gap height has the dimensional form [20], [22]:

$$\varepsilon_0\,\varepsilon_{T1s}(\varphi,\,\vartheta_1) = \varepsilon_{Ts}(\varphi,\,\vartheta_1)$$
$$\equiv \Delta\varepsilon_x\cos\varphi\sin\vartheta_1 + \Delta\varepsilon_y\sin\varphi\sin\vartheta_1 - \Delta\varepsilon_z\cos\vartheta_1 - R$$
$$+ [(\Delta\varepsilon_x\cos\varphi\sin\vartheta_1 + \Delta\varepsilon_y\sin\varphi\sin\vartheta_1 - \Delta\varepsilon_z\cos\vartheta_1)^2$$
$$+ (R+\varepsilon_{\min})(R+2D+\varepsilon_{\min})]^{0.5}. \qquad (5)$$

3. Governing equations

Synovial fluid flow in the gap of human hip joint is described by the equations of conservation of momentum and the equation of continuity. These equations

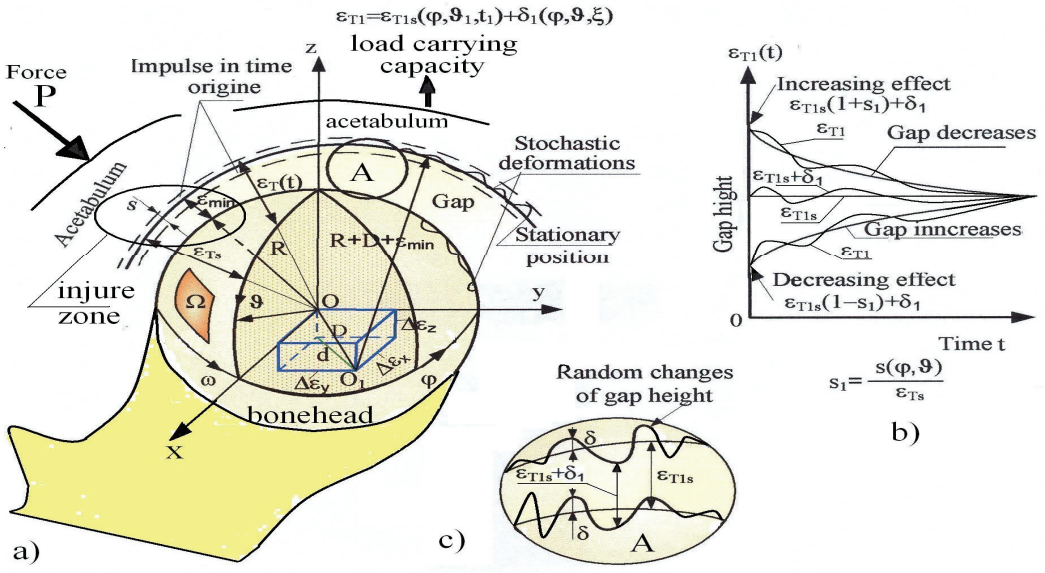

Fig. 3. The geometry of bone head and hip joint gap:
(a) lubrication region, eccentricities, gap height variations in the time after injury, (b) gap height variations after injury,
(c) stochastic deformations of cartilage, effects of impact and random roughness

We assume the centre of spherical bone head to be at the point O(0, 0, 0) and the centre of spherical acetabulum at the point $O_1(x-\Delta\varepsilon_x,\, y-\Delta\varepsilon_y,\, z+\Delta\varepsilon_z)$. The eccentricity has the value D (see figure 3). Symbols $\Delta\varepsilon_x$, $\Delta\varepsilon_y$, $\Delta\varepsilon_z$ denote components of eccentricities in x, y, z directions.

The dimensionless function $s_1 = s(\varphi,\,\vartheta_{1s})/\varepsilon_{Ts}(\varphi,\,\vartheta_1)$ for $\vartheta_{1s} \equiv \vartheta_s/R$, $\vartheta_1 \equiv \vartheta/R$ describes the gap-height changes during the impulsive motion caused by the applied force P (see figure 1a and figure 3a). The gap height increases if $s_1 > 0$, and decreases if $s_1 < 0$.

The symbol ω_0 denotes an angular velocity in s^{-1} and describes the changes of time perturbations in unsteady flow of synovial fluid in the joint gap-height direction.

If t_1 increases, then for $s_1 > 0$ the enlarged gap-height decreases, and in a sufficiently long time after impulse it attains the same time-independent value ε_{Ts}. If the dimensionless time t_1 increases, then for $s_1 < 0$ the reduced gap-height increases. In a sufficiently long time after impulse the gap attains the same time-independent value ε_{Ts} (see figure 3).

and the second-order approximation of the general constitutive equation, given by Rivlin and Ericksen, can be written in the form [13]:

$$\mathrm{Div}\,\boldsymbol{S} = \rho\boldsymbol{a}, \quad \mathrm{div}\,\boldsymbol{v} = 0,$$
$$\boldsymbol{S} = -p\boldsymbol{I} + \eta\boldsymbol{A}_1 + \alpha\boldsymbol{A}_1^2 + \beta\boldsymbol{A}_2, \qquad (6)$$

where:

$\boldsymbol{S}$ – the stress tensor,

p – pressure,

$\boldsymbol{I}$ – the unit tensor,

$\boldsymbol{A}_1$ and $\boldsymbol{A}_2$ – the first two Rivlin–Ericksen tensors,

η, α, β – three material constants, where $\eta = \eta_0\eta_1$ denotes dynamic viscosity in Pas, and α, β are pseudo-viscosity coefficients in Pas^2,

ρ – synovial fluid density, $\mathrm{kg/m}^3$.

Tensors $\boldsymbol{A}_1$ and $\boldsymbol{A}_2$ are given by symmetric matrices defined by [6], [12], [13]:

$$\boldsymbol{A}_1 \equiv \boldsymbol{L} + \boldsymbol{L}^T, \quad \boldsymbol{A}_2 \equiv \mathrm{grad}\,\boldsymbol{a} + (\mathrm{grad}\,\boldsymbol{a})^T + 2\boldsymbol{L}^T\boldsymbol{L},$$
$$\boldsymbol{a} \equiv \boldsymbol{L}\,\boldsymbol{v} + \frac{\partial v}{\partial t}, \qquad (7)$$

where:

$\boldsymbol{L}$ – tensor of fluid velocity gradient vector in s^{-1},

$\boldsymbol{L}^{\boldsymbol{T}}$ – tensor for transpose of a matrix of gradient vector of a synovial fluid in s^{-1},

$\boldsymbol{v}$ – velocity vector in m/s,

t – time in s,

$\boldsymbol{a}$ – acceleration vector, m/s^2.

It is assumed that the product of Deborah and Strouhal numbers, i.e., *DeStr* and the product of Reynolds number, dimensionless clearance, and Strouhal number, i.e., *Re*ψ*Str* are of the same order. We additionally assume rotational motion of human bone head with the peripheral velocity $U = \omega R$, unsymmetrical, synovial unsteady flow in the gap, viscoelastic properties of synovial fluid, constant value of the synovial fluid density ρ, characteristic dimensional value of the gap height of hip joint, ε_0, no slip on the cartilage surfaces, R – radius of bone head, ω – angular velocity of bone head [16], [18]. We assume the relations between dimensional and dimensionless quantities to be in the following form [16]:

$$r = \varepsilon_0 r_1, \quad \vartheta = R\vartheta_1, t = t_0 t_1, \quad \varepsilon_T = \varepsilon_0 \varepsilon_{T1},$$
$$v_\varphi = UV_{\varphi\Sigma}, \quad v_r \equiv U\psi V_{r\Sigma}, \quad v_\vartheta \equiv UV_{\vartheta\Sigma}, \quad p = p_0 p_1,$$
$$p_0 \equiv U\eta_o R/(\varepsilon_0)^2, \tag{8}$$

and the Reynolds numbers, modified Reynolds numbers, Strouhal and Deborah numbers are as follows [16]:

$$Re \equiv \rho U\varepsilon_0/\eta_0, \quad Re\psi \equiv \rho\omega(\varepsilon_0)^2/\eta_0, \quad Str \equiv R/Ut_0,$$
$$De \equiv \beta U/\eta_0 R, \tag{9}$$
$$DeStr = \beta/\eta_0 t_0, \quad Re\psi Str = \rho(\varepsilon_0)^2/\eta_0 t_0.$$

The pseudo-viscosity β appearing in the inequality $0 < \beta/t_0 < \eta_0$, valid for synovial fluid has mostly values from 0.000001 to 0.001000 Pas^2. The dimensionless symbols have the lower index "1". Neglecting the terms of the radial clearance $\psi \equiv \varepsilon_0/R \approx 10^{-3}$ in the governing equations expressed in the spherical coordinates: r, φ, ϑ, and taking into account the above mentioned assumptions, we have [18], [22]:

$$Re\psi Str\frac{\partial V_{\varphi\Sigma}}{\partial t_1} = -\frac{1}{\sin\vartheta_1}\frac{\partial p_1}{\partial\varphi} + \frac{\partial}{\partial r_1}\left(\frac{\partial V_{\varphi\Sigma}}{\partial r_1}\right) + DeStr\frac{\partial^3 V_{\varphi\Sigma}}{\partial t_1 \partial r_1^2}, \tag{10}$$

$$0 = \frac{\partial p_1}{\partial r_1}, \tag{11}$$

$$Re\psi Str\frac{\partial V_{\vartheta\Sigma}}{\partial t_1} = -\frac{\partial p_1}{\partial\vartheta_1} + \frac{\partial}{\partial r_1}\left(\frac{\partial V_{\vartheta\Sigma}}{\partial r_1}\right) + DeStr\frac{\partial^3 V_{\vartheta\Sigma}}{\partial t_1 \partial r_1^2}, \tag{12}$$

$$\frac{\partial V_{\varphi\Sigma}}{\partial\varphi} + \sin(\vartheta_1)\frac{\partial V_{r\Sigma}}{\partial r_1} + \frac{\partial}{\partial\vartheta_1}[V_{\vartheta\Sigma}\sin(\vartheta_1)] = 0, \tag{13}$$

where:

$0 \le \varphi \le 2\pi\theta_1$, $0 \le \theta_1 \le 1$, $\pi/8 \le \vartheta_1 \le \pi/2$, $0 \le r_1 \le \varepsilon_{T1}$,

ε_{T1} – dimensionless total gap height,

$V_{\phi\Sigma}$, $V_{r\Sigma}$, $V_{\vartheta\Sigma}$ – dimensionless synovial fluid velocity components in circumferential, gap height and meridian directions of the bone head, respectively.

p_1 – unknown dimensionless pressure.

Analytical integration method of partial differential system (10)–(13) is presented in Appendix sections A1, A2. The solutions of synovial fluid velocity components in hip joint gap have been derived in Appendix sections A1, A2.

3. Stochastic Reynolds equation

If we put synovial fluid velocity components (A15) into continuity equation (A22), then we obtain dimensionless pressure function and its corrections: p_{10}, p_{11}, ... For example, if we put expressions (A16), (A17) into $(A22)_0$ and take the expected values of both sides of equation $(A22)_0$, then the following modified Reynolds equation determines unknown pressure function p_{10}:

$$\frac{\sqrt{\pi}}{2N_\varepsilon^2}\frac{1}{\sin\vartheta_1}E\left\{\frac{\partial}{\partial\varphi}\left[J(\varepsilon_{T1}N_\varepsilon^2)\frac{\partial p_{10}}{\partial\varphi}\right]\right\}$$
$$+\frac{\sqrt{\pi}}{2N_\varepsilon^2}E\left\{\frac{\partial}{\partial\vartheta_1}\left[J(\varepsilon_{T1}N_\varepsilon^2)\frac{\partial p_{10}}{\partial\vartheta_1}\sin\vartheta_1\right]\right\}$$
$$= -(\sin\vartheta_1)E\left\{\frac{\partial}{\partial\varphi}H(\varepsilon_{T1}N_\varepsilon)\right\} - Str\frac{\partial E(\varepsilon_{T1})}{\partial t_1}\sin\vartheta_1, \tag{14}$$

where:

$$J(\varepsilon_{T1}N_\varepsilon) \equiv W_{ef}(\varepsilon_{T1}N_\varepsilon)Y_0(\varepsilon_{T1}N_\varepsilon) - \int_0^{\varepsilon_{T1}} Y_0(r_1 N_\varepsilon)dr_1,$$
$$H(\varepsilon_{T1}N_\varepsilon) \equiv \varepsilon_{T1} - W_{ef}(\varepsilon_{T1}N_\varepsilon), \tag{15}$$

$$W_{ef}(\varepsilon_{T1}N_\varepsilon) \equiv \frac{\int_0^{\varepsilon_{T1}} erf(r_1 N_\varepsilon)dr_1}{erf(\varepsilon_{T1}N_\varepsilon)}, \qquad (16a)$$

$$N_\varepsilon \equiv \frac{1}{2}\sqrt{\frac{Re\psi Str}{t_1}},$$

$$Y_0(r_1N_\varepsilon) = \frac{2}{\sqrt{\pi}}\int_0^{r_1N_\varepsilon}\left(e^{\chi_1^2}\int_0^{\chi_1}e^{-\chi_2^2}d\chi_2\right)d\chi_1 - \frac{2}{\sqrt{\pi}}\int_0^{r_1N_\varepsilon}e^{-\chi_1^2}d\chi_1\int_0^{r_1N_\varepsilon}e^{\chi_1^2}d\chi_1, \qquad (16b)$$

and $\varepsilon_{T1} = \varepsilon_{T1s}(\varphi, \vartheta_1, t_1) + \delta_1$, $0 \le r_2 \le r_1 \le \varepsilon_{T1}$, $0 \le \varphi < 2\pi\theta_1$, $0 \le \theta_1 < 1$, $\pi/8 \le \vartheta_1 \le \pi/2$, $0 \le t_1 < \infty$, $0 \le \chi_2 \le \chi_1 \le \varepsilon_{T1}N_\varepsilon$, $0 \le N_\varepsilon(t_1) = 0.5(Res/t_1)^{0.5} < \infty$.

The modified Reynolds equation (14) determines an unknown time-dependent pressure function $p_{10}(\varphi, \vartheta_1, t_1)$ with stochastic changes. We obtain a convenient form of equation (14) for numerical calculations and demonstration of probability terms by using the optimum function of probability density distribution, for the stochastic gap-height changes caused by the vibration and unsteady load [20]. The mean value of total film thickness $E(\varepsilon_{T1})$ and the mean value of pressure function $E(p_{10})$ can be calculated by virtue of the expectancy operator defined in equations (2), (3). Finally, we can write equation (14) in the form:

$$\frac{\sqrt{\pi}}{2N_\varepsilon^2}\frac{1}{\sin\vartheta_1}\frac{\partial}{\partial\varphi}\left\{\int_{-c_1}^{+c_1}\left[\left(1-\frac{\delta_1^2}{c_1^2}\right)^5 J(\varepsilon_{T1}N_\varepsilon)\right]d\delta_1\frac{\partial p_{10}}{\partial\varphi}\right\}$$

$$+\frac{\sqrt{\pi}}{2N_\varepsilon^2}\frac{\partial}{\partial\vartheta_1}\left\{\int_{-c_1}^{+c_1}\left[\left(1-\frac{\delta_1^2}{c_1^2}\right)^5 J(\varepsilon_{T1}N_\varepsilon)\right]d\delta_1\frac{\partial p_{10}}{\partial\vartheta_1}\sin\vartheta_1\right\}$$

$$=-(\sin\vartheta_1)\frac{\partial}{\partial\varphi}\left\{\int_{-c_1}^{+c_1}\left(1-\frac{\delta_1^2}{c_1^2}\right)^5 H(\varepsilon_{T1}N_\varepsilon)d\delta_1\right\}$$

$$-Str\frac{\partial}{\partial t_1}\left[\int_{-c_1}^{+c_1}\left(1-\frac{\delta_1^2}{c_1^2}\right)^5(\varepsilon_{T1s}+\delta_1)d\delta_1\right]\sin\vartheta_1 \qquad (17)$$

where $-c_1 \le \delta_1 \le c_1$, $0 \le \varphi \le 2\pi$, $\pi/8 \le \vartheta_1 \le \pi/2$. We obtain a more convenient form of equation (17) by expanding the function J and H into the Taylor series in the neighborhood of the point $\delta_1 = 0$ in the following form:

$$J(\varepsilon_{T1}N_\varepsilon) = J(\varepsilon_{T1s}N_\varepsilon) + \frac{\delta_1}{1!}\left(\frac{\partial J(\varepsilon_{T1}N_\varepsilon)}{\partial\delta_1}\right)_{\delta_1=0} + \frac{\delta_1^2}{2!}\left(\frac{\partial^2 J(\varepsilon_{T1}N_\varepsilon)}{\partial\delta_1^2}\right)_{(\delta_1=0)} + \ldots, \qquad (18)$$

$$H(\varepsilon_{T1}N_\varepsilon) = \varepsilon_{T1s} - W_{ef}(\varepsilon_{T1s}N_\varepsilon) + \frac{\delta_1}{1!}\left(\frac{\partial H(\varepsilon_{T1}N_\varepsilon)}{\partial\delta_1}\right)_{\delta_1=0} - \frac{\delta_1^2}{2!}\left(\frac{\partial^2 W_{ef}(\varepsilon_{T1}N_\varepsilon)}{\partial\delta_1^2}\right)_{\delta_1=0} + \ldots \qquad (19)$$

We put series (18), (19) in equation (17). Integrating the series term by term with respect to the variable δ_1 in equation (17), we obtain the following form of stochastic Reynolds equation:

$$\frac{\sqrt{\pi}}{2N_\varepsilon^2}\frac{1}{\sin\vartheta_1}\frac{\partial}{\partial\varphi}\left[K(\varepsilon_{T1}N_\varepsilon)\frac{\partial p_{10}}{\partial\varphi}\right] + \frac{\sqrt{\pi}}{2N_\varepsilon^2}\frac{\partial}{\partial\vartheta_1}\left[K(\varepsilon_{T1}N_\varepsilon)\frac{\partial p_{10}}{\partial\vartheta_1}\sin\vartheta_1\right]$$

$$=-(\sin\vartheta_1)\frac{\partial}{\partial\varphi}\left[\varepsilon_{T1s} - W_{ef}(\varepsilon_{T1s}N_\varepsilon) - \frac{\sigma_{s1}^2}{2!}\frac{\partial^2 W_{ef}(\varepsilon_{T1}N_\varepsilon)}{\partial\delta_1^2}(\delta_1=0) + \ldots\right]$$

$$-Str\frac{\partial\varepsilon_{T1s}}{\partial t_1}\sin\vartheta_1. \qquad (20)$$

The integration performed enables us to show kernel function $K(\varepsilon_{T1}N_\varepsilon)$ in the following form:

$$K(\varepsilon_{T1}N_\varepsilon) = J(\varepsilon_{T1s}N_\varepsilon) + \frac{\sigma_{s1}^2}{2!}\left(\frac{\partial^2 J(\varepsilon_{T1}N_\varepsilon)}{\partial\delta_1^2}\right)_{\delta_1=0} + \ldots, \qquad (21)$$

where:

$$\left(\frac{\partial^2 J(\varepsilon_{T1}N_\varepsilon)}{\partial\delta_1^2}\right)_{\delta_1=0} = \left(\frac{\partial^2 W_{ef}(\varepsilon_{T1}N_\varepsilon)}{\partial\delta_1^2}\right)_{\delta_1=0} Y_0(\varepsilon_{T1s}N_\varepsilon) + 2\left(\frac{\partial W_{ef}(\varepsilon_{T1}N_\varepsilon)}{\partial\delta_1}\right)_{\delta_1=0}\left(\frac{\partial Y_0(\varepsilon_{T1}N_\varepsilon)}{\partial\delta_1}\right)_{\delta_1=0} + \left(\frac{\partial^2 Y_0(\varepsilon_{T1}N_\varepsilon)}{\partial\delta_1^2}\right)_{\delta_1=0} W_{ef}(\varepsilon_{T1s}N_\varepsilon) - \left(\frac{\partial Y_0(\varepsilon_{T1}N_\varepsilon)}{\partial\delta_1}\right)_{\delta_1=0}, \qquad (22)$$

whereas function Y_0 and its derivatives are as follows:

$$Y_0(\varepsilon_{T1s}N_\varepsilon)=\frac{2}{\sqrt{\pi}}\int_0^{\varepsilon_{T1s}N_\varepsilon}\left(e^{\chi_1^2}\int_0^{\chi_1}e^{-\chi_2^2}d\chi_2\right)d\chi_1$$

$$-\frac{2}{\sqrt{\pi}}\int_0^{\varepsilon_{T1s}N_\varepsilon}e^{-\chi_1^2}d\chi_1\int_0^{\varepsilon_{T1s}N_\varepsilon}e^{\chi_1^2}d\chi_1, \tag{23}$$

and

$$\left(\frac{\partial Y_0(\varepsilon_{T1}N_\varepsilon)}{\partial\delta_1}\right)_{\delta_1=0}$$

$$=\frac{-2N_\varepsilon}{\sqrt{\pi}}e^{-N_\varepsilon^2\varepsilon_{T1s}^2}\int_0^{\varepsilon_{T1s}N_\varepsilon}e^{\chi_1^2}d\chi_1, \tag{24}$$

and

$$\left(\frac{\partial^2 Y_0(\varepsilon_{T1}N_\varepsilon)}{\partial\delta_1^2}\right)_{\delta_1=0}$$

$$=\frac{-2N_\varepsilon^2}{\sqrt{\pi}}+\frac{4N_\varepsilon^3}{\sqrt{\pi}}\varepsilon_{T1s}e^{-N_\varepsilon^2\varepsilon_{T1s}^2}\int_0^{\varepsilon_{T1s}N_\varepsilon}e^{\chi_1^2}d\chi_1. \tag{25}$$

First derivative of function W_{ef} occurring in expansion (22) has the following form:

$$\left(\frac{\partial W_{ef}(\varepsilon_{T1}N_\varepsilon)}{\partial\delta_1}\right)_{\delta_1=0}$$

$$=1-W_{ef}^*(\varepsilon_{T1s}N_\varepsilon)W_{ef}(\varepsilon_{T1s}N_\varepsilon), \tag{26}$$

and using the definition of *erf* function we have:

$$W_{ef}(\varepsilon_{T1s}N_\varepsilon)\equiv\frac{\int_0^{\varepsilon_{T1s}}\left(\int_0^{N_\varepsilon r_1}e^{-\chi_1^2}d\chi_1\right)dr_1}{N_\varepsilon\varepsilon_{T1s}\int_0^{}e^{-\chi_1^2}d\chi_1},$$

$$W_{ef}^*(\varepsilon_{T1s}N_\varepsilon)\equiv\frac{N_\varepsilon\exp(-N_\varepsilon^2\varepsilon_{T1s}^2)}{N_\varepsilon\varepsilon_{T1s}\int_0^{}e^{-\chi_1^2}d\chi_1}. \tag{27}$$

Second partial derivative of function W_{ef} occurring in r.h.s. of (20) has the following form:

$$\left(\frac{\partial^2 W_{ef}(\varepsilon_{T1}N_\varepsilon)}{\partial\delta_1^2}\right)_{\delta_1=0}=-W_{ef}^*(\varepsilon_{T1s}N_\varepsilon)$$

$$+2[N_\varepsilon^2\varepsilon_{T1s}+W_{ef}^*(\varepsilon_{T1s}N_\varepsilon)]$$

$$W_{ef}^*(\varepsilon_{T1s}N_\varepsilon)W_{ef}(\varepsilon_{T1s}N_\varepsilon). \tag{28}$$

4. Limit forms of stochastic Reynolds equations

If t_1 tends to infinity, i.e., N_ε tends to zero, then equation (20) tends to the classical Reynolds equation but for random conditions. To explain this fact we use the limits obtained after application of the Hospital rule and presented by equations (A23)–(A31) in Appendix intersection A3. We put such limits into series expansion of kernel function K in equation (20). Hence equation (20) tends, for $N_\varepsilon\to 0$, to the following form:

$$\frac{1}{\sin\vartheta_1}\frac{\partial}{\partial\varphi}\left\{\left[\left(-\frac{\varepsilon_{T1s}^2}{2}\right)\frac{\varepsilon_{T1s}}{2}-\int_0^{\varepsilon_{T1s}}\left(-\frac{r_1^2}{2}\right)dr_1\right.\right.$$

$$\left.\left.+\frac{\sigma_{s1}^2}{2!}\left(\frac{\varepsilon_{T1s}^2}{2}\times 0-2\varepsilon_{T1s}\times\frac{1}{2}+\frac{\varepsilon_{T1s}}{2}(-1)-(-\varepsilon_{T1s})\right)\right]\frac{\partial p_{10}}{\partial\varphi}\right\}$$

$$+\frac{\partial}{\partial\vartheta_1}\left\{\left[\left(-\frac{\varepsilon_{T1s}^2}{2}\right)\frac{\varepsilon_{T1s}}{2}-\int_0^{\varepsilon_{T1s}}\left(-\frac{r_1^2}{2}\right)dr_1\right.\right.$$

$$\left.\left.+\frac{\sigma_{s1}^2}{2!}\left(\frac{\varepsilon_{T1s}^2}{2}\times 0-2\varepsilon_{T1s}\times\frac{1}{2}+\frac{\varepsilon_{T1s}}{2}(-1)-(-\varepsilon_{T1s})\right)\right]\right.$$

$$\left.\times\frac{\partial p_{10}}{\partial\vartheta_1}\sin\vartheta_1\right\}$$

$$=-(\sin\vartheta_1)\frac{\partial}{\partial\varphi}\left[\int_0^{\varepsilon_{T1}}\left(1-\frac{r_1}{\varepsilon_{T1s}}\right)dr_1+\frac{\sigma_{s1}^2}{2!}\times 0\right]$$

$$-Str\frac{\partial(\varepsilon_{T1s})}{\partial t_1}\sin\vartheta_1. \tag{29}$$

After final calculations, we obtain the following form of the classical Reynolds equations in the spherical coordinates but for random conditions:

$$\frac{1}{\sin\vartheta_1}\frac{\partial}{\partial\varphi}\left[(\varepsilon_{T1s}^3+3\sigma_{s1}^2\varepsilon_{T1s})\frac{\partial p_{10}}{\partial\varphi}\right]$$

$$+\frac{\partial}{\partial\vartheta_1}\left[(\varepsilon_{T1s}^3+3\sigma_{s1}^2\varepsilon_{T1s})\frac{\partial p_{10}}{\partial\vartheta_1}\sin\vartheta_1\right]$$

$$=6\frac{\partial\varepsilon_{T1s}}{\partial\varphi}\sin\vartheta_1, \tag{30}$$

where $0 \le \varphi < 2\pi\theta_1$, $0 \le \theta_1 < 1$, $\pi/8 \le \vartheta_1 \le \pi/2$.

Equation (30) determines the time-independent pressure function with stochastic changes. If the standard deviation tends to zero ($\sigma_{s1} \to 0$), then equation (30) tends to the known classical Reynolds equation for stationary flow without random conditions.

5. Load carrying capacity

The dimensional carrying capacities in spherical bearing are calculated from the following formula:

$$C=\frac{\omega\eta_0 R^2}{\psi^2}\sqrt{\left[\int_{\pi/8}^{\pi/2}\left(\int_0^{\varphi_k}p_1(\varphi,\vartheta_1,t_1)(\sin\varphi)\sin\vartheta_1 d\varphi\right)d\vartheta_1\right]^2+\left[\int_{\pi/8}^{\pi/2}\left(\int_0^{\varphi_k}p_1(\varphi,\vartheta_1,t_1)(\cos\varphi)\sin\vartheta_1 d\varphi\right)d\vartheta_1\right]^2} \tag{31}$$

where symbol φ_k denotes the end coordinate of the film in circumferential direction and $0 \le \varphi < 2\pi\theta_1$, $0 \le \theta_1 < 1$, $\pi/8 \le \vartheta_1 \le \pi/2$, $\vartheta = R\vartheta_1$. Dimensionless pressure has the following form:

$$p_1(\varphi,\vartheta_1,t_1)=p_{10}(\varphi,\vartheta_1,t_1)$$

$$+Gp_{11}(\varphi,\vartheta_1,t_1)+G^2p_{12}(\varphi,\vartheta_1,t_1)$$

$$+\ldots+G^n p_{1n}(\varphi,\vartheta_1,t_1)+\ldots \tag{32}$$

for $G \equiv \beta/(\eta_0 t)$.

6. Pressure correction for unsteady visco-elastic synovial fluid properties

The dimensionless values of pressure corrections caused by the unsteady, visco-elastic, non-Newtonian properties of synovial fluid, are as follows:

$$\sum_{n=1}^{\infty}G^n p_{1n}(\varphi,\vartheta_1,t_1)$$

$$=Gp_{11}(\varphi,\vartheta_1,t_1)+G^2p_{12}(\varphi,\vartheta_1,t_1)$$

$$+\ldots+G^n p_{1n}(\varphi,\vartheta_1,t_1)+\ldots \tag{33}$$

From semi-numerical calculations it follows that the above-mentioned pressure corrections in lubrication region $\Omega(\varphi, \vartheta_1, t_1)$ described by the following inequalities $\{0 \le \varphi < \pi;\ \pi/8 \le \vartheta_1 \le \pi/2;\ 10 \le t_1 \le 10^8\}$, can be estimated by the following inequality:

$$p_{1n}(\varphi,\vartheta_1,t_1) \le n \quad \text{for} \quad n=1,2,3,\ldots \tag{34}$$

Combining equations (33), (34), we obtain:

$$\sum_{n=1}^{\infty}G^n p_{1n}(\varphi,\vartheta_1,t_1) \le \sum_{n=1}^{\infty}nG^n. \tag{35}$$

For $0 < G < 1$ the infinite series in r.h.s. of inequality (35) is convergent and has the sum:

$$\sum_{n=1}^{\infty}nG^n=\frac{G}{(1-G)^2}\equiv M. \tag{36}$$

The expression (36) presents the upper estimation of the sum of infinite terms of pressure corrections caused by the unsteady, visco-elastic, non-Newtonian properties of synovial fluid.

The ratio M_R of the M value to max p_{10} the maximum value of pressure for unsteady, Newtonian properties of synovial fluid has the following form:

$$M_R \equiv \frac{M}{\max p_{10}}. \tag{37}$$

7. Results of numerical calculations

In the case of impulsive motion there are determined the dimensionless pressure p_{10} and its dimensionless corrections: p_{11}, p_{12}, … in the lubrication

region $\Omega(\varphi,\ \vartheta_1,\ t_1)$ described by the following inequalities $\{0 \le \varphi < \pi;\ \pi/8 \le \vartheta_1 \le \pi/2; 10 \le t_1 \le 10^8\}$. The pressure $p_{10}, p_{11}, p_{12}, \ldots$ is determined by virtue of the modified Reynolds equations (14), (17), (20), (30), $(A22)_1$, $(A22)_2$ taking into account the gap height (4), (5) and unified calculation algorithm in section A4. Numerical calculations are performed in Matlab 7.2 and Mathcad 12 Professional Program by means of the recurrence equations and unified summation algorithm [18] for: the radius of spherical bone head R = 0.0265 m, angular velocity of the impulsive perturbations of gap height ω_0 = 0.15 s^{-1}, characteristic dimensional time t_0 = 0.000001 s. The gap height (4), (5) is taken into account, where the following eccentricities of bone head: $\Delta\varepsilon_x$ = 4.0 μm, $\Delta\varepsilon_y$ = 0.5 μm, $\Delta\varepsilon_z$ = 3.0 μm, are assumed. In the calculations we take the optimum dimensionless standard deviation σ_{s1} = 0.375. We assume that the dynamic viscosity of synovial fluid has the value of η_0 = 0.50 Pas, pseudo-viscosity coefficient β = 0.0000005 Pas^2, density of synovial fluid ρ = 1010 kg/m^3, angular velocity of spherical bone head ω = 1.5 s^{-1}, the minimum value of gap height $\min(\varepsilon_{T1s})$ changes within the time interval of 0.00001 s ≤ t ≤ 100 s, and it attains values within

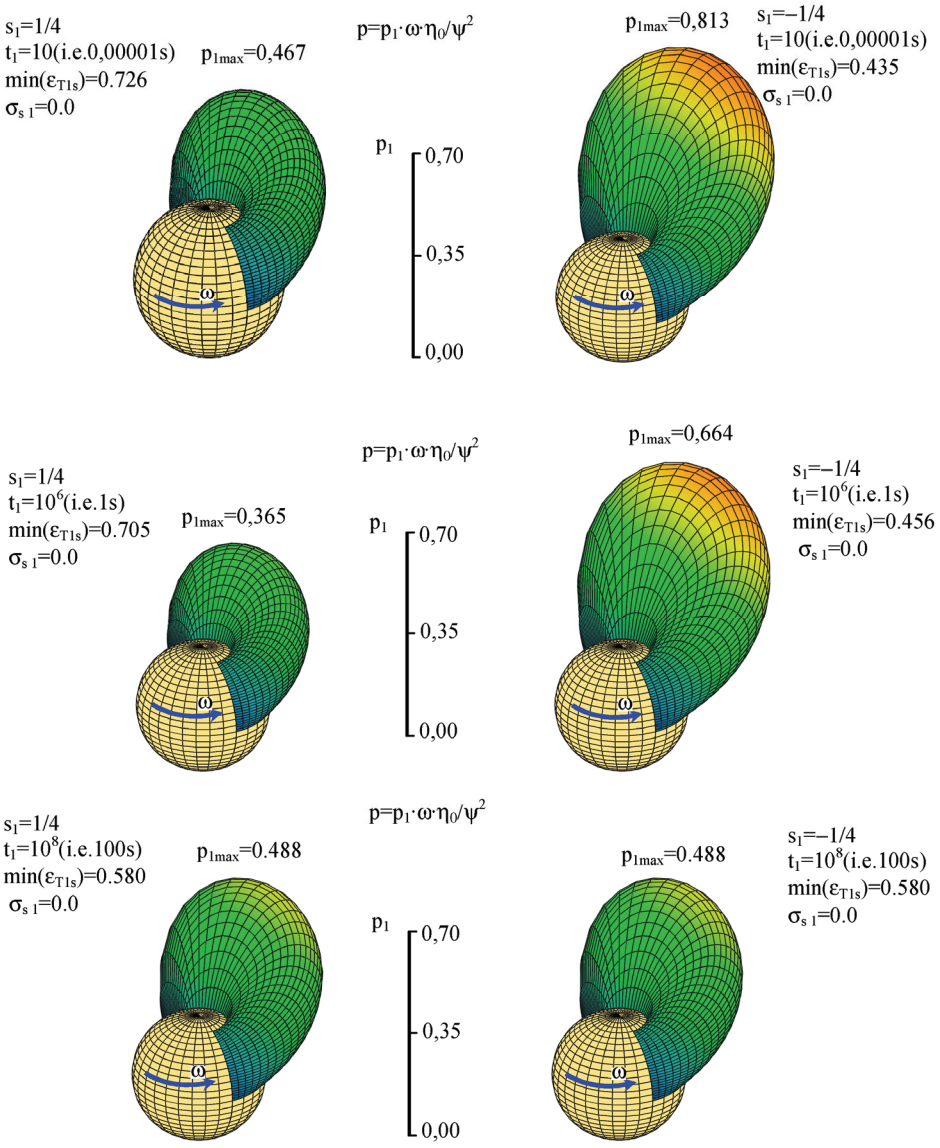

Fig. 4. The dimensionless hydrodynamic total pressure p_1 distributions inside the gap of human spherical hip joint in the region Ω: $0 \le \varphi \le \pi$, $\pi R/8 \le \vartheta \le \pi R/2$ without stochastic changes (σ_{s1} = 0) in the dimensionless times: t_1 = 10 (i.e., t = 0.00001 s), $t_1 = 10^6$ (i.e., t = 1 s), $t_1 = 10^8$ (i.e., t = 100 s), after the impulse moment, for the increasing (decreasing) effects of gap-height changes – see the left (right) column of the figures, respectively. The results are obtained for the following data: R = 0.0265 m; η_0 = 0.50 Pas; ρ = 1010 kg/m^3; ε_0 = 10 μm, β = 0.0000005 Pas^2, $\Delta\varepsilon_x$ = 4 μm; $\Delta\varepsilon_y$ = 0.5 μm; $\Delta\varepsilon_z$ = 3 μm; $\psi \equiv \varepsilon_0/R = 3.774 \cdot 10^{-4}$; ω = 1.5 s^{-1}; ω_0 = 0.15s^{-1}; Str = 666666; $Re \cdot \psi \cdot Str$ = 0.202; $De \cdot Str$ = 1.000

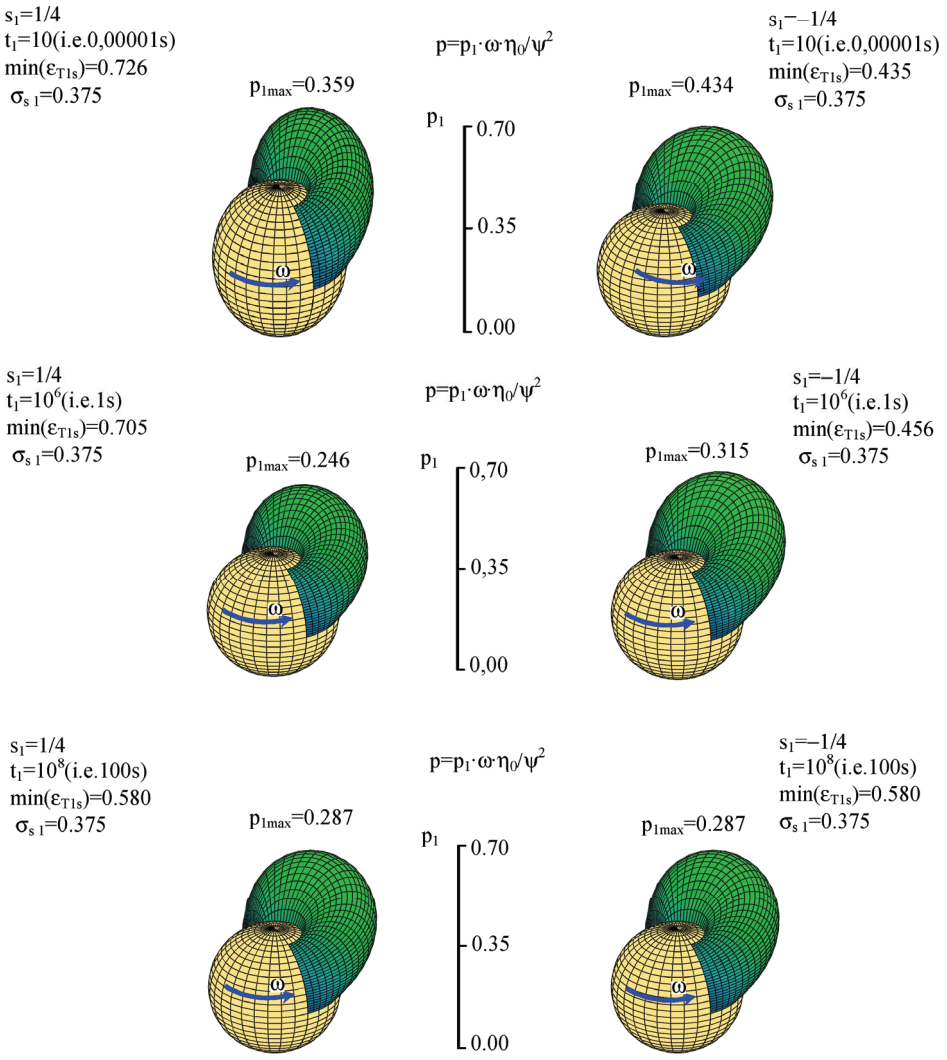

Fig. 5. The dimensionless hydrodynamic total pressure p_1 distributions inside the gap of human spherical hip joint in the region Ω: $0 \le \varphi \le \pi$, $\pi R/8 \le \vartheta \le \pi R/2$ for stochastic changes with the standard deviation $\sigma_{s1} = 0.375$ (i.e., 0.37 μm) in the dimensionless times: $t_1 = 10$ (i.e., $t = 0.00001$ s), $t_1 = 10^6$ (i.e., $t = 1$ s), $t_1 = 10^8$ (i.e., $t = 100$ s), after the impulse moment, for the increasing (decreasing) effects of gap-height changes, see the left (right) column of the figures, respectively. The results are obtained for the following data: $R = 0.0265$ m; $\eta_0 = 0.50$ Pas; $\beta = 0{,}0000005$ Pas^2, $\rho = 1010$ kg/m^3; $\varepsilon_0 = 10$ μm; $\Delta\varepsilon_x = 4$ μm; $\Delta\varepsilon_y = 0.5$ μm; $\Delta\varepsilon_z = 3$ μm; $\psi \equiv \varepsilon/R \approx 3.774 \cdot 10^{-4}$; $\omega = 1{,}5$ s^{-1}; $\omega_0 = 0{,}15$ s^{-1}; $Str = 666666$; $Re \cdot \psi \cdot Str = 0.202$; $De \cdot Str = 1.000$

the range from 4.35 μm to 7.26 μm. The average relative radial clearance has the value of $\psi \equiv \varepsilon_0/R = 3.774 \cdot 10^{-4}$. The characteristic dimensional pressure $p_0 = \omega\eta_0/\psi^2$ attains the value of 5.267 MPa. The characteristic dimensional gap-height value equals $\varepsilon_0 = 10$ μm and the Strouhal number $Str = 666666$, $Re \cdot \psi \cdot Str = 0.202$, $De \cdot Str = 1.000$. In this case we have $0 \le \beta/\eta_0 t < 1$. For the dimensionless times: $t_1 = 10$, $t_1 = 10^6$, $t_1 = 10^8$, i.e., for the dimensional times: $t = 0.00001$ s; $t = 1.0$ s; $t = 100.0$ s, respectively, and for $s_1 = \pm 0.25$ we obtain the distributions of dimensionless pressure given in figures 4 and 5. To obtain real values of time we must multiply the dimensionless values t_1 by the characteristic time value $t_0 = 0.000001$ s. For example, $t_1 = 10^6$ denotes 1 s after impulse. To obtain a dimensional value of pressure we must multiply the dimensionless pressure values (see figures 4 and 5) by the characteristic pressure value p_0. Figure 4 presents the dimensionless pressure values without random effects for $\sigma_{s1} = 0$. The dimensionless pressure values presented in figure 5 are obtained for stochastic gap-height changes for $\sigma_{s1} = 0.375$. The distributions of dimensionless total pressure presented for $s_1 > 0$ on the left-hand side of figures 4 and 5, are obtained for the enlargement effect of gap-height caused by impulsive motion. In this case, if the time after the impulse increases, then the gap height decreases and total pressure decreases and increases, and in a sufficiently long time after impulse it tends to the time-independent pressure.

The pressure distributions presented for $s_1 < 0$ on the right-hand side in figures 4 and 5 are obtained for the reduced effects of gap height caused by impulsive motion. In this case, if the time after the impulse increases, then the gap height increases and the total pressure decreases and in a sufficiently long times after impulse it tends to the time-independent pressure.

In the following time instants after the moment of injury, namely: $t = 0.000005$ s (i.e., $t_1 = 5$); $t = 0.00001$ s (i.e., $t_1 = 10$), $t = 0.001$ s (i.e., $t_1 = 1000$); $t = 1$ s (i.e., $t_1 = 1000\ 000$); $t = 100$ s (i.e., $t_1 = 100\ 000\ 000$), we have: $G = 0.200\ 000\ 000$; $G = 0.100\ 000\ 000$; $G = 0.010\ 000\ 000$; $G = 0.000\ 001\ 000$; $G = 0.000\ 000\ 010$, respectively. For the above time instants the upper estimations M of maximum pressure caused by the unsteady, viscoelastic synovial fluid properties have the following values: $M = 0.312\ 500\ 000$; $M = 0.123\ 456\ 000$; $M = 0.010\ 203\ 000$; $M = 0.000\ 001\ 000$; $M = 0.000\ 000\ 0010$, respectively.

In the case of increase (decrease) changes of gap after injury, the ratio defined in equation (37) without stochastic changes for $\sigma_{s1} = 0$ and with stochastic changes for $\sigma_{s1} = 0.375$, has the following values:

$$M_R(\sigma_{s1} = 0) = 0.357558\,(0.178260);$$

$$M_R(\sigma_{s1} = 0.375) = 0.521186(0.395498);$$

$$\text{for} \quad t = 10^{-5}\ \text{s},$$

$$M_R(\sigma_{s1} = 0) = 2.7 \cdot 10^{-6}(1.5 \cdot 10^{-6});$$

$$M_R(\sigma_{s1} = 0.375) = 3.78 \cdot 10^{-6}(3.17 \cdot 10^{-6});$$

$$\text{for} \quad t = 1\,\text{s},$$

$$M_R(\sigma_{s1} = 0) = 2.05 \cdot 10^{-8}(2.05 \cdot 10^{-8}),$$

$$M_R(\sigma_{s1} = 0.375) = 3.78 \cdot 10^{-8}(3.78 \cdot 10^{-8})$$

$$\text{for} \quad t = 100\,\text{s}.$$

In the case of increase (decrease) changes of the gap after injury, the dimensionless maximum total pressure for viscoelastic properties of synovial fluid, without stochastic changes for $\sigma_{s1} = 0$ and with stochastic changes for $\sigma_{s1} = 0.375$, is presented in table 1.

Now, in figures 6–8, there are determined the dimensionless pressure p_{10} and capacity values for unsteady flow and Newtonian synovial fluid properties only. Calculations are performed in the lubrication region $\Omega(\varphi,\ \vartheta_1,\ t_1)$ described by the following inequalities $\{0 \le \varphi < \pi;\ \pi/8 \le \vartheta_1 \le \pi/2;\ 1 \le t_1 \le 10^7\}$. The pressure p_{10} is determined by virtue of the modified Reynolds equations (14), (17), (20), (30) taking into account the gap height (4), (5) and unified calculation algorithm presented in Appendix section A4. Numerical calculations are performed in Matlab 7.2 and Mathcad 12 Professional Program by means of the recurrence equations and unified summation algorithm [18] for: the radius of spherical bone head $R = 0.0265$ m, angular velocity of the impulsive perturbations of gap height $\omega_0 = 0.08\ \text{s}^{-1}$, characteristic dimensional time $t_0 = 0.00001$ s. The gap height (4), (5) is taken into account, where the following eccentricities of bone head: $\Delta\varepsilon_x = 2.5$ μm, $\Delta\varepsilon_y = 0.5$ μm, $\Delta\varepsilon_z = 2.0$ μm, are assumed. In the calculations, we take the optimum dimensionless standard deviation $\sigma_{s1} = 0.375$. We assume that the dynamic viscosity of synovial fluid has the value of $\eta_0 = 0.35$ Pas, density of synovial fluid $\rho = 1010\ \text{kg/m}^3$, angular velocity of spherical bone head $\omega = 1.3\ \text{s}^{-1}$, the minimum value of gap height $\min(\varepsilon_{T1s})$ changes within the time interval of $0.00001\ \text{s} \le t \le 100$ s, and it attains values within the range from 4.50 μm to 6.97 μm. The average relative radial clearance has the value of $\psi \equiv \varepsilon_0/R = 3.774 \cdot 10^{-4}$. The characteristic dimensional pressure $p_0 = \omega\eta_0/\psi^2$ attains the value of 3.195 MPa. The characteristic dimensional gap-height value equals $\varepsilon_0 = 10$ μm and the Strouhal number $Str = 76923$, $Re \cdot \psi \cdot Str = 0.029$, $De \cdot Str = 0.571$. In this case, we have $0 \le \beta/\eta_0 t < 1$. For the dimensionless times: $t_1 = 1$, $t_1 = 10^5$, $t_1 = 10^7$, i.e., for the dimensional times: $t = 0.00001$ s; $t = 1.0$ s; $t = 100.0$ s, respectively, and for $s_1 = \pm 0.22$ we obtain the distributions of dimensionless pressure given in figures 6 and 7. To obtain real values of time we must multiply the dimensionless values t_1 by the

Table 1. Dimensionless maximum total pressure $p_{1\max}$ for non-Newtonian viscoelastic properties

Dimensional time t	$P_{1\max}$			
	$\sigma_{s1} = 0.000$ without random changes		$\sigma_{s1} = 0.375$ with random changes	
	gap increases	gap decreases	gap increases	gap decreases
$t = 0.00001$ s	0.467	0.813	0.3598	0.4340
$t = 1.0000$ s	0.365	0.664	0.2460	0.3150
$t = 100.0000$ s	0.488	0.488	0.287	0.287

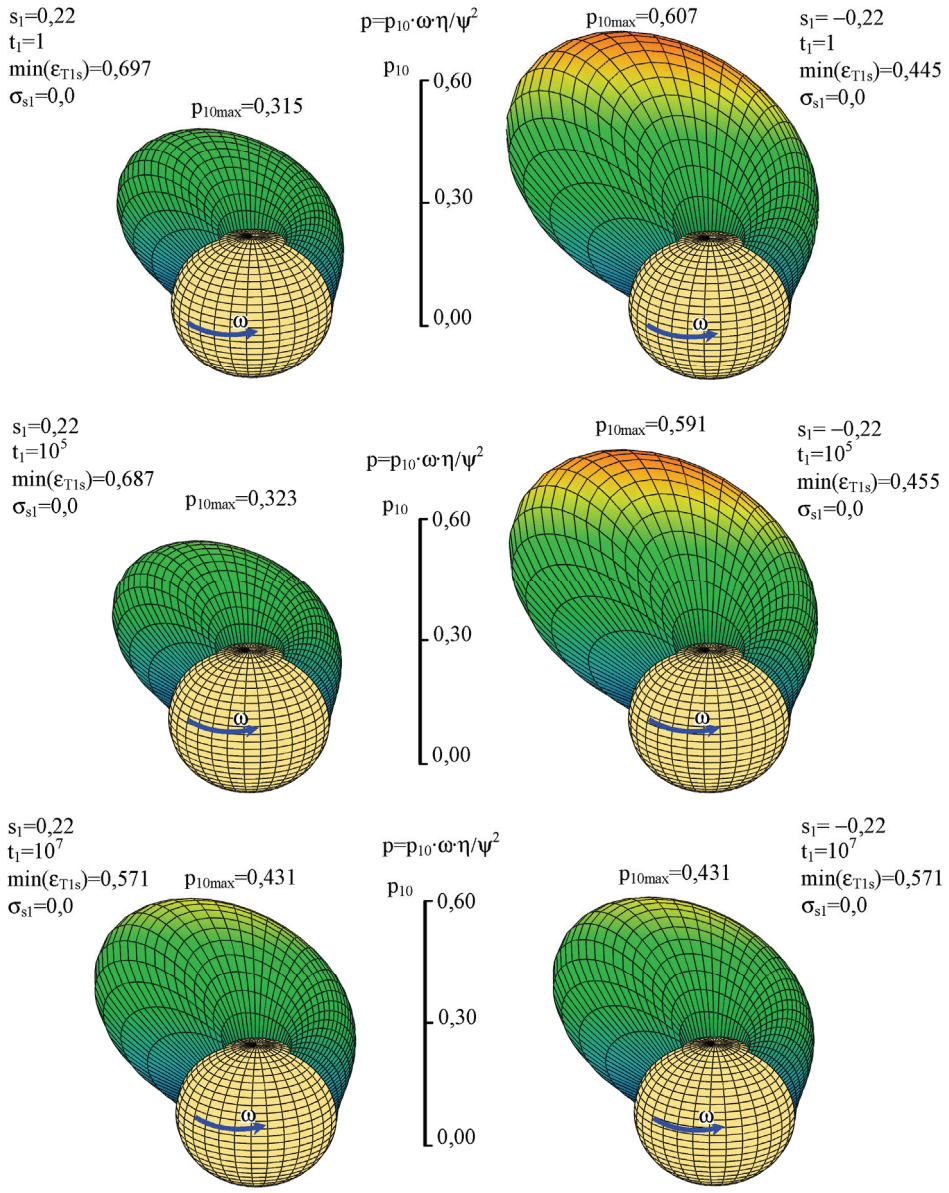

Fig. 6. The dimensionless hydrodynamic total pressure p_{10} distributions inside the gap of human spherical hip joint in the region Ω: $0 \le \varphi \le \pi$, $\pi R/8 \le \vartheta \le \pi R/2$ without stochastic changes ($\sigma_{s1} = 0$) in the dimensionless times: $t_1 = 1$ (i.e., $t = 0.00001$ s), $t_1 = 10^5$ (i.e., $t = 1$ s), $t_1 = 10^7$ (i.e., $t = 100$ s), after the impulse moment, for the increasing (decreasing) effects of gap-height changes, see the left (right) column of the figures, respectively. The results are obtained for the following data: $R = 0.0265$ m; $\eta_0 = 0.35$ Pas; $\rho = 1010$ kg/m^3; $\Delta\varepsilon_x = 2.5$ μm; $\Delta\varepsilon_y = 0.5$ μm; $\Delta\varepsilon_z = 2$ μm; $\psi \equiv \varepsilon/R \approx 3.774 \cdot 10^{-4}$; $\omega = 1.3$ s^{-1}; $\omega_0 = 0.08$ s^{-1}; $Str = 76923$; $Re \cdot \psi \cdot Str = 0.029$; $De \cdot Str = 0.571$

characteristic time value $t_0 = 0.00001$ s. For example, $t_1 = 10^5$ denotes 1 s after impulse. To obtain a dimensional value of pressure we must multiply the dimensionless pressure values (see figure 6, figure 7) by the characteristic pressure value p_0. Figure 6 presents the dimensionless pressure values without random effects for $\sigma_{s1} = 0$. The dimensionless pressure values presented in figure 7 are obtained for stochastic gap-height changes for $\sigma_{s1} = 0.375$. The distributions of dimensionless total pressure presented for $s_1 > 0$ on the left-hand side of figures 6 and 7 are obtained for the enlargement effect of gap-height caused by impulsive motion. In this case, if the time after the impulse increases, then the gap height decreases and total pressure decreases and increases, and in a sufficiently long time after impulse it tends to the time-independent pressure.

The pressure distributions presented for $s_1 < 0$ on the right-hand side in figures 6 and 7 are obtained for the reduced effects of gap height caused by impulsive motion. In this case, if the time after the impulse increases, then the gap height increases and the total pressure decreases and in a sufficiently long times after impulse it tends to the time-independent pressure.

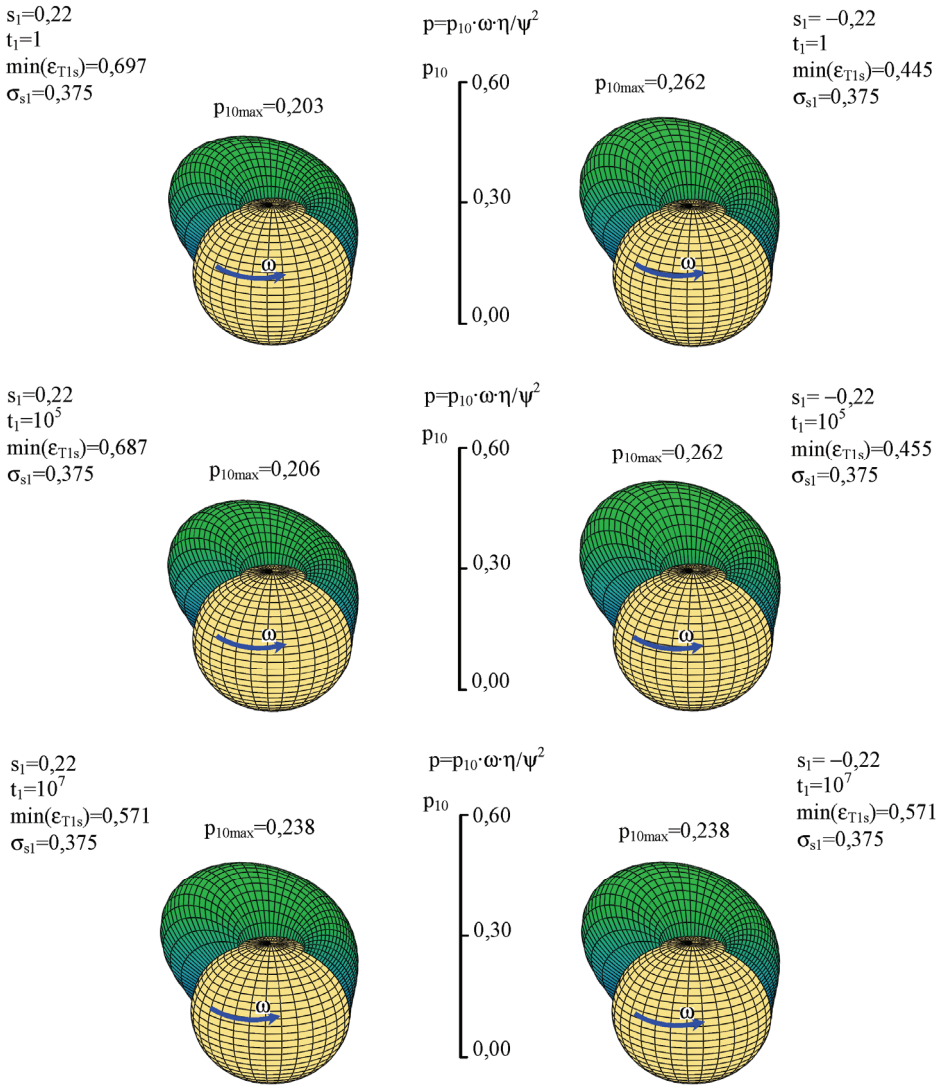

Fig. 7. The dimensionless hydrodynamic total pressure p_{10} distributions inside the gap of human spherical hip joint in the region Ω: $0 \le \varphi \le \pi$, $\pi R/8 \le \vartheta \le \pi R/2$ for stochastic changes with the standard deviation $\sigma_{s1} = 0.375$ (i.e., 0.37 μm) in the dimensionless times: $t_1 = 1$ (i.e., $t = 0.00001$ s), $t_1 = 10^5$ (i.e., $t = 1$ s), $t_1 = 10^7$ (i.e., $t = 100$ s), after the impulse moment, for the increasing (decreasing) effects of gap-height changes see the left (right) column of the figures, respectively. The results are obtained for the following data: $R = 0.0265$ m; $\eta_0 = 0.35$ Pas; $\rho = 1010$ kg/m^3; $\Delta\varepsilon_x = 2.5$ μm; $\Delta\varepsilon_y = 0.5$ μm; $\Delta\varepsilon_z = 2$ μm; $\psi \equiv \varepsilon/R \approx 3.774 \cdot 10^{-4}$; $\omega = 1.3$ s^{-1}; $\omega_0 = 0.08$ s^{-1}; $Str = 76923$; $Re \cdot \psi \cdot Str = 0.029$; $De \cdot Str = 0.571$

Table 2. Dimensionless maximum total pressure $p_{10\max}$ for Newtonian properties

Dimensional time t	$P_{1\max}$			
	$\sigma_{s1} = 0.000$ without random changes		$\sigma_{s1} = 0.375$ with random changes	
	gap increases	gap decreases	gap increases	gap decreases
$t = 0.00001$ s	0.315	0.607	0.2030	0.2620
$t = 1.0000$ s	0.323	0.591	0.2060	0.2520
$t = 100.0000$ s	0.431	0.431	0.238	0.2380

In the case of increase (decrease) changes of gap after injury, the dimensionless maximum pressure for Newtonian properties of synovial fluid, without stochastic changes for $\sigma_{s1} = 0$ and with stochastic changes for $\sigma_{s1} = 0.375$, is presented in table 2.

Figure 8 presents the dimensional value of capacity for Newtonian synovial fluid properties versus the dimensional time ranging from the beginning of the impulse to 100 s after the impulse. The viscoelastic synovial fluid properties are neglected here ($\beta = 0$).

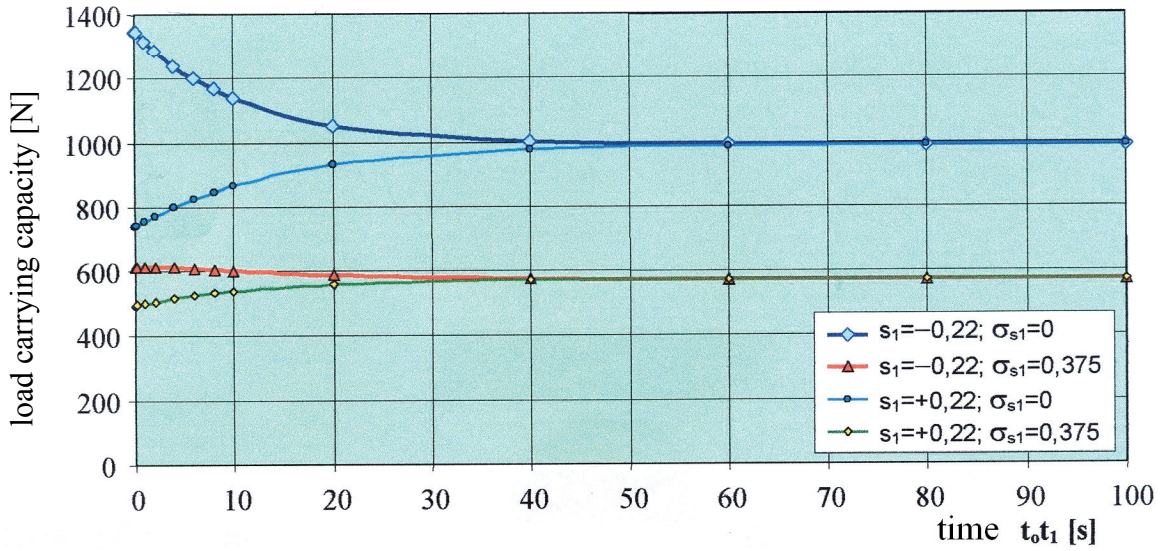

Fig. 8. The dimensional values of capacity C versus the dimensional time in the range from 10^{-5} second to 100 seconds after impulse inside the gap of human spherical hip joint in the region Ω: $0 \le \varphi \le \pi$, $\pi R/8 \le \vartheta \le \pi R/2$ for stochastic changes of roughness of cartilage surface with the standard deviation $\sigma_{s1} = 0.375$ (i.e., 0.37 μm) and without random effects for $\sigma_{s1} = 0$. The results are obtained for the following data: $R = 0.0265$ m; $\eta_0 = 0.35$ Pas; $\rho = 1010$ kg/m^3; $\Delta\varepsilon_x = 2.5$ μm; $\Delta\varepsilon_y = 0.5$ μm; $\Delta\varepsilon_z = 2$ μm; $\psi \equiv \varepsilon/R \approx 3.774 \cdot 10^{-4}$; $\omega = 1.3$ s^{-1}; $\omega_0 = 0.08$ s^{-1}; $Str = 76923$; $Re \cdot y \cdot Str = 0.029$; $De \cdot Str = 0.571$

8. Conclusions

◇ The new results presented in this paper refer to the determination of the influences of the unsteady, visco-elastic, non-Newtonian properties of synovial fluid on the hydrodynamic pressure in very short time after injury in human joint.

At the moment of injury ($t = 0$) the pressure function has undeterminable point. The limit value of the pressure function cannot be determined in a numerical way. Therefore, such values in the neighborhood of point $t = 0$ are not realistic. From analytical and numerical calculations it follows that the largest changes and increases of the hydrodynamic pressure distributions caused by the aforementioned viscoelastic properties of synovial fluid in human hip joint arise in some microseconds after the moment of injury and attain about 35 percent.

Several seconds after the moment of injury the influences of the viscoelastic synovial fluid properties on the pressure distribution are already negligibly small.

◇ If the trauma increases the gap height ($s_1 > 0$) of a normal joint, then in the time just after impulse the gap height decreases and the total pressure at first decreases and then increases. In a sufficiently long time after impulse the gap height and the pressure attains the time-independent values.

If the trauma decreases the gap height ($s_1 < 0$), then in the time after impulse the gap height increases and the total pressure decreases. In a sufficiently long time after impulse the gap height and the pressure attain the time-independent values.

◇ If the time after the impulse moment is long enough, i.e., for $t_1 \to \infty$, and if we take the optimum standard deviations of gap height, then the pressure distributions tend to the identical pressure distributions for the increasing ($s_1 > 0$) and decreasing ($s_1 < 0$) effects of the gap-height changes caused by the impulse. This limit pressure distribution can also be obtained from the stochastic Reynolds equation (30) for arbitrary standard deviation σ_{s1}.

◇ From the numerical calculations we conclude that some microseconds after impulse the pressure of the human hip joint, obtained for stochastic effects with the optimum standard deviation $\sigma_{s1} = 0.375$, decreases by about 50% in comparison with the pressure and capacity obtained for smooth cartilage surface without asperities and random effects.

The limit values of pressure function in the long time after impulse ($t \to \infty$) are well determined and calculated. In a long time after impulse the above-mentioned decreases of pressure with stochastic effects are about 30 percent only.

◇ The numerical calculations show that for the Newtonian properties of synovial fluid, the largest changes of load carrying capacities in human hip joint arise within the time interval from 0.1 s to 30 s after impulse during the unsteady motion.

Acknowledgements

This paper was supported by the BW/10/9025826/09 founds. Moreover, the author thanks for the financial help of the Polish Ministerial Grant 3475/B/T02/2009/36 in the years 2009–2012.

References

[1] CWANEK J., *The usability of the surface geometry parameters for the evaluation of artificial hip joint wear*, (in Polish), Rzeszów University Publisher, 2009.

[2] DOWSON D., *Bio-Tribology of Natural and Replacement Synovial Joints*, [in:] C. Van Mow, A. Ratcliffe, S.L-Y. Woo, *Biomechanics of Diarthrodial Joint*, Springer-Verlag, New York–Berlin–Londyn–Paris–Tokyo–Hong Kong, 1990, Vol. 2, Chap. 29, 305–345.

[3] FISZ M., *Probability Theory and Mathematical Statistics*, John Wiley & Sons, Inc., New York, 1963.

[4] FUNG Y.C., *Biomechanics: Mechanical Properties of Living Tissues*, Springer Verlag, New York, 1993.

[5] FUNG Y.C., *A First Course in Continuum Mechanics: for physical and biological engineers and scientists*, 3-rd ed., Englewood Cliffs, N.J. Prentice-Hall, 1994.

[6] FUNG Y.C., *Biomechanics, Motion, Flow, Stress and Growth*, Springer Verlag, New York–Hong Kong, 1990.

[7] GARCIA J.J., ALTIERO N.J., HAUT R.C., *Estimation of in Situ Elastic Properties of Biophasic Cartilage Based on a Transversely Isotropic Hypo-Elastic Model*, Journal of Biomechanical Engineering, February 2000, Vol. 122, 1–8.

[8] JEMIOŁO S., TELEGA J.J., MICHALAK C., *Hyperelastic Anisotropic Model of Soft Tissues Acta Bioeng*, Biomechanics, 2000, 2 Suppl. 1, 235–240.

[9] KNOLL V.D., *Trans-scaphoid perilunate fracture dislocations*, J. Hand Surg. Am., 2005, 30A, 1145–1152.

[10] MOW V.C, RATCLIFFE A., WOO S., *Biomechanics of Diarthrodial Joints*, Springer Verlag, Berlin–Heidelberg–New York, 1990.

[11] PAWLAK Z., URBANIAK W., OLOYEDE A., *The relationship between friction and wettability in aqueous environment*, Wear, 171, 2011, 1745–1749.

[12] TEIPEL I., *The Impulsive Motion of a Flat Plate in a Viscoelastic Fluid*, Springer Verlag, Acta Mechanica, 1981, 39, 277–279.

[13] TRUESDELL C.A., *First Course in Rational Continuum Mechanics*, Maryland, John Hopkins University, Baltimore, 1972.

[14] WIERZCHOLSKI K., *Oil velocity and pressure distribution in short journal bearing under Rivlin Ericksen lubrication*, System Analysis Modeling and Simulations OPA Overseas Publishers. Assoc. N.V., 1998, Vol. 32, 205–228.

[15] WIERZCHOLSKI K., *The method of solutions for hydrodynamic lubrication by synovial fluid flow in human joint gap*, Control and Cybernetics, 2002, Vol. 31, No. 1, 91–116.

[16] WIERZCHOLSKI K., *Comparison between impulsive and periodic non Newtonian lubrication of human hip joint*, Engineering Transactions, 2005, 53, 1, 69–114.

[17] WIERZCHOLSKI K., MISZCZAK A., *Load Carrying Capacity of Microbearings with Parabolic Journal*, Solid State Phenomena, Trans. Technical Publications, Switzerland, Vol. 147–149, 2009, 542–547.

[18] WIERZCHOLSKI K., *Topology of calculating pressure and friction coefficients for time-dependent human hip joint lubrication*, Acta of Bioengineering and Biomechanics, 2011, Vol. 13, No. 1, 41–56.

[19] WIERZCHOLSKI K., *Algorithm for Friction Force Computation in Intelligent Micro-Pairs System*, (in English), XIII Journal of Applied Computer Science, 2011, Vol. 19, No. 1, 139–160.

[20] WIERZCHOLSKI K., NOWAKOWSKA K., *Pseudo-Gaussian density function for gap height between two surfaces*, (in English), XIII Journal of Applied Computer Science, 2010, Vol. 18, No. 2, 79–90.

[21] WIERZCHOLSKI K., CWANEK J., *Measurements of head surfaces of endoprosthesis*, Proceedings of 7th International Symposium INSYCONT '06, Cracow, 2006, 49–54.

[22] WIERZCHOLSKI K., *Bio and slide bearings: their lubrication by non-Newtonian fluids and application in non conventional systems*, *Vol. II: The theory of human joint unsteady lubrication*, Monograph (pp. 1–172), Published by Krzysztof Wierzcholski, Gdańsk University of Technology, ISBN 83-923367-0-4, Gdańsk, 2006.

[23] WIERZCHOLSKI K., *Hip joint lubrication after injury for stochastic description with optimum standard deviation*, Acta of Bioengineering and Biomechanics, (in English), 2005, Vol. 7, No. 2, 51–78.

[24] WIERZCHOLSKI K., *Non-Newtonian lubrication of human hip joint for unsteady impulsive motion*, Exploitation Problems of Machines Polish Academy of Sciences (Zagadnienia Eksploatacji Maszyn Kwartalnik PAN), Nr. 1, 2006, Vol. 41, 37–60.

[25] www.knoll.j.orthopeadics research

A. Appendix: Analytical Integration Method of Hydrodynamic Problem

A1. The method of integration applied to hydrodynamic problem

We introduce a new dimensionless variable [18]:

$$\chi \equiv r_1 N_\varepsilon, \qquad t_1 > 0, \qquad 0 < \frac{DeStr}{t_1} = \frac{\beta}{\eta_0 t} \equiv G < 1, \tag{A1}$$

and we assume solutions of the system (10)–(13) to be in the form of the following convergent series [18], [22]:

$$V_{\varphi\Sigma} = v_{\varphi 0}(\chi, \varphi, \vartheta_1) + \frac{DeStr}{t_1} v_{\varphi 1}(\chi, \varphi, \vartheta_1) + \left(\frac{DeStr}{t_1}\right)^2 v_{\varphi 2}(\chi, \varphi, \vartheta_1) + \ldots, \tag{A2}$$

$$V_{\vartheta\Sigma} = v_{\vartheta 0}(\chi,\varphi,\vartheta_1) + \frac{DeStr}{t_1} v_{\vartheta 1}(\chi,\varphi,\vartheta_1) + \left(\frac{DeStr}{t_1}\right)^2 v_{\vartheta 2}(\chi,\varphi,\vartheta_1) + \ldots, \tag{A3}$$

$$V_{r\Sigma} = v_{r0}(\chi,\varphi,\vartheta_1) + \frac{DeStr}{t_1} v_{r1}(\chi,\varphi,\vartheta_1) + \left(\frac{DeStr}{t_1}\right)^2 v_{r2}(\chi,\varphi,\vartheta_1) + \ldots, \tag{A4}$$

$$p_1 = p_{10}(\varphi,\vartheta_1,t_1) + \frac{DeStr}{t_1} p_{11}(\varphi,\vartheta_1,t_1) + \left(\frac{DeStr}{t_1}\right)^2 p_{12}(\varphi,\vartheta_1,t_1) + \ldots, \tag{A5}$$

where: $t_1 > 0$, $0 < DeStr \ll 1$, $(DeStr/t_1) < 1$.

In equations (10)–(13), we replace the derivatives with respect to the variables t_1, r_1 by the derivatives with respect of one variable χ only, using the following relations [22]:

$$\frac{\partial}{\partial t_1} = \frac{\partial}{\partial \chi}\frac{\partial \chi}{\partial t_1} = -\frac{1}{4}\sqrt{Res}\,\frac{r_1}{t_1\sqrt{t_1}}\frac{\partial}{\partial \chi} = -\frac{\chi}{2t_1}\frac{\partial}{\partial \chi}, \tag{A6}$$

$$\frac{\partial^2}{\partial r_1^2} = \frac{\partial}{\partial r_1}\left(\frac{\partial}{\partial r_1}\right) = \frac{\partial}{\partial \chi}\left(\frac{\partial}{\partial \chi}\frac{\partial \chi}{\partial r_1}\right)\frac{\partial \chi}{\partial r_1} = \frac{Res}{4t_1}\frac{\partial^2}{\partial \chi^2}, \tag{A7}$$

$$\frac{\partial^3}{\partial t_1 \partial r_1^2} = \frac{\partial}{\partial t_1}\left(\frac{Res}{4t_1}\frac{\partial^2}{\partial \chi^2}\right) = -\frac{Res}{4t_1^2}\frac{\partial^2}{\partial \chi^2} + \frac{Res}{4t_1}\frac{\partial}{\partial \chi}\left(\frac{\partial^2}{\partial \chi^2}\right)\frac{\partial \chi}{\partial t_1} = -\frac{Res}{4t_1^2}\left(\frac{\partial^2}{\partial \chi^2} + \frac{\chi}{2}\frac{\partial^3}{\partial \chi^3}\right) \tag{A8}$$

where: $Res \equiv Re\,\psi Str$.

Afterwards, we put the series (A2)–(A5) into the changed system (10)–(13), where the variables t_1, r_1 are replaced by the variable χ. Moreover, we equate the terms multiplied by the same powers of the parameter $(DeStr/t_1)^k$ for $k = 0, 1, 2, \ldots$ Thus we obtain the sequence of systems of ordinary differential equations [18]:

$$\frac{d^2 v_{\varphi 0}}{d\chi^2} + 2\chi\frac{dv_{\varphi 0}}{d\chi} = \frac{4\nu t}{\varepsilon_o^2 \sin(\vartheta_1)}\frac{\partial p_{10}}{\partial \varphi},$$

$$\frac{d^2 v_{\vartheta 0}}{d\chi^2} + 2\chi\frac{dv_{\vartheta 0}}{d\chi} = \frac{4\nu t}{\varepsilon_o^2}\frac{\partial p_{10}}{\partial \vartheta_1}, \tag{A9}$$

$$\frac{d^2 v_{\varphi 1}}{d\chi^2} + 2\chi\frac{dv_{\varphi 1}}{d\chi} + 4v_{\varphi 1} = \frac{4\nu t}{\varepsilon_o^2 \sin(\vartheta_1)}\frac{\partial p_{11}}{\partial \varphi} + \frac{d^2 v_{\varphi 0}}{d\chi^2} + \frac{1}{2}\chi\frac{d^3 v_{\varphi 0}}{d\chi^3},$$

$$\frac{d^2 v_{\vartheta 1}}{d\chi^2} + 2\chi\frac{dv_{\vartheta 1}}{d\chi} + 4v_{\vartheta 1} = \frac{4\nu t}{\varepsilon_o^2}\frac{\partial p_{11}}{\partial \vartheta_1} + \frac{d^2 v_{\vartheta 0}}{d\chi^2} + \frac{1}{2}\chi\frac{d^3 v_{\vartheta 0}}{d\chi^3}, \tag{A10}$$

$$\frac{d^2 v_{\varphi 2}}{d\chi^2} + 2\chi\frac{dv_{\varphi 2}}{d\chi} + 8v_{\varphi 2} = \frac{4\nu t}{\varepsilon_o^2 \sin(\vartheta_1)}\frac{\partial p_{12}}{\partial \varphi} + 2\frac{d^2 v_{\varphi 1}}{d\chi^2} + \frac{1}{2}\chi\frac{d^3 v_{\varphi 1}}{d\chi^3},$$

$$\frac{d^2 v_{\vartheta 2}}{d\chi^2} + 2\chi\frac{dv_{\vartheta 2}}{d\chi} + 8v_{\vartheta 2} = \frac{4\nu t}{\varepsilon_o^2}\frac{\partial p_{12}}{\partial \vartheta_1} + 2\frac{d^2 v_{\vartheta 1}}{d\chi^2} + \frac{1}{2}\chi\frac{d^3 v_{\vartheta 1}}{d\chi^3}, \tag{A11}$$

$$\ldots\ldots\ldots\ldots\ldots\ldots\ldots\ldots\ldots\ldots,$$

where: $0 \le \chi \equiv r_1 N_\varepsilon < \varepsilon_1 N_\varepsilon$, $0 < r_1 < \varepsilon_1$, $0 < \varphi < 2\pi$, $\pi R/8 \le \vartheta \le \pi R/2$, $\vartheta_1 = \vartheta/R$.

$$\chi \equiv \frac{r}{2\sqrt{\nu t}} = r_1 N_\varepsilon,\ N_\varepsilon \equiv \frac{\varepsilon_0}{2\sqrt{\nu t}},\ \nu \equiv \frac{\eta_0}{\rho},$$
$$t > 0,\ 0 < \frac{\beta}{\eta_0 t} < 1,\ 0 < r_1 < \varepsilon_1,\ r = \varepsilon_0 r_1. \tag{A12}$$

The synovial fluid velocity components of $v_{\varphi k}$, $v_{\vartheta k}$, v_{rk} and pressure p_{1k} for $k = 0$ depend on the time and synovial fluid dynamic viscosity but they are independent of the viscoelastic properties. Flow parameters for $k = 1, 2, \ldots$ describe corrections of synovial fluid velocity components and pressure caused by the time dependent viscoelastic properties of synovial

fluid. The functions: $v_{\varphi k}$, $v_{\vartheta k}$, p_{1k} and quantities χ, N_ε are dimensionless.

A2. Boundary conditions and particular solutions

The spherical bone head moves in the circumferential direction φ only. Hence the synovial fluid velocity components on the bone head surface in the circumferential direction equals the peripheral velocity of spherical surface of bone head. These velocity values are changing in the meridian direction ϑ according to the variations of function sin(*). The peripheral velocity in the circumferential direction on the pole of bone head has zero value for $\vartheta_1 = 0$ and on the equator of spherical bone has dimensionless value 1 for $\vartheta_1 = \pi/2$. The synovial fluid velocity component on spherical bone head surface in the meridian direction ϑ equals zero, because the spherical bone head is motionless in ϑ direction.

Viscous synovial fluid flows around the bone head. Hence, on the bone head surface the synovial fluid velocity component in the gap-height direction equals zero.

The spherical acetabulum surface is motionless in the circumferential and meridian directions. Thus the synovial fluid velocity components on the acetabulum surface are equal to zero in the circumferential and meridian directions. But the spherical bone head does not sustain any changes in gap height direction. Hence the gap height changes with time. Therefore the synovial fluid velocity component in the gap height direction r equals the first derivative of the gap-height with respect to the time.

The corrections of values of the synovial fluid velocity components cannot change the above presented boundary conditions which are assumed on the bone head and acetabulum surface in the circumferential, meridian and gap height directions. Therefore for the synovial fluid velocity components and their corrections we have the following boundary conditions [18]:

$$\begin{gathered} r = 0, \quad \chi = 0, \quad v_{\varphi 0} = \sin\vartheta_1, \\ v_{\varphi 1} = 0, \quad \ldots, \quad v_{\varphi k} = 0, \ldots, \\ r = 0, \quad \chi = 0, \quad v_{\vartheta 0} = 0, \\ v_{\vartheta 1} = 0, \quad \ldots, \quad v_{\vartheta k} = 0, \ldots, \\ r = 0, \quad \chi = 0, \quad v_{r0} = 0, \\ v_{r1} = 0, \quad \ldots, \quad v_{rk} = 0, \ldots, \end{gathered} \tag{A13}$$

$$\begin{gathered} r = \varepsilon, \quad \chi = N_\varepsilon \varepsilon_1, \quad v_{\varphi 0} = 0, \\ v_{\varphi 1} = 0, \quad \ldots, \quad v_{\varphi k} = 0, \ldots, \\ r = \varepsilon, \quad \chi = N_\varepsilon \varepsilon_1, \quad v_{\vartheta 0} = 0, \\ v_{\vartheta 1} = 0, \quad \ldots, \quad v_{\vartheta k} = 0, \ldots, \\ r = \varepsilon, \quad \chi = N_\varepsilon \varepsilon_1, \quad v_{r0} = Str\partial\varepsilon_1/\partial t_1, \\ v_{r1} = 0, \quad \ldots, \quad v_{rk} = 0, \ldots, \end{gathered} \tag{A14}$$

with $Str \equiv 1/\omega_0 t_0$, $t_1 = t/t_0$ and $k = 1, 2, 3, \ldots$

For $\beta = 0$ one obtains an equation for the original Reynolds problem.

Solutions of equations (A9)–(A11), ... have been found in closed form. Imposing the boundary conditions (A13), (A14) on the general solutions of the differential equations (A9)–(A11), ..., we finally obtain the following particular solutions [22]:

$$v_{\varphi 0}, \quad v_{\varphi 1}, \quad v_{\varphi 2}, \quad \ldots \quad v_{\vartheta 0}, \quad v_{\vartheta 1}, \quad v_{\vartheta 2}, \ldots \tag{A15}$$

For example, in the zero step ($k = 0$) from (A9) we obtain velocity components $v_{\varphi 0}$, $v_{\vartheta 0}$ in the circumferential and meridian directions for unsteady Newtonian fluid flow in impulsive motion in the following form:

$$\begin{aligned} v_{\varphi 0}(\varphi, r_1, \vartheta_1, t_1) &= +\sin\vartheta_1 \\ &- \left\{ \sin\vartheta_1 - \frac{\sqrt{\pi}}{2N_\varepsilon^2 \sin\vartheta_1} \frac{\partial p_{10}}{\partial \varphi} Y_0(\chi = N_\varepsilon \varepsilon_1) \right\} \\ &\times \frac{erf(r_1 N_\varepsilon)}{erf(\varepsilon_1 N_\varepsilon)} - \frac{\sqrt{\pi}}{2N_\varepsilon^2 \sin\vartheta_1} \frac{\partial p_{10}}{\partial \varphi} Y_0(\chi = N_\varepsilon r_1), \end{aligned} \tag{A16}$$

$$\begin{aligned} v_{\vartheta 0}(\varphi, r_1, \vartheta_1, t_1) &= \frac{\sqrt{\pi}}{2N_\varepsilon^2} \frac{\partial p_{10}}{\partial \vartheta_1} Y_0(\chi = N_\varepsilon \varepsilon_1) \\ &\times \frac{erf(r_1 N_\varepsilon)}{erf(\varepsilon_1 N_\varepsilon)} - \frac{\sqrt{\pi}}{2N_\varepsilon^2} \frac{\partial p_{10}}{\partial \vartheta_1} Y_0(\chi = N_\varepsilon r_1), \end{aligned} \tag{A17}$$

with

$$\begin{aligned} Y_0(\chi) &\equiv \int_0^\chi e^{\chi_1^2} erf\chi_1 d\chi_1 - erf\chi \int_0^\chi e^{\chi_1^2} d\chi_1, \\ erf\chi_1 &\equiv \frac{2}{\sqrt{\pi}} \int_0^{\chi_1} \exp(-\chi_2^2) d\chi_2, \end{aligned} \tag{A18}$$

and $0 \le t_1 < \infty$, $0 \le r_1 \le \varepsilon_1$, $b_{m1} \le \vartheta_1 \le b_{s1}$, $0 < \varphi < 2\pi\theta_1$, $0 \le \theta_1 < \infty$, $0 \le \chi_2 \le \chi_1 \le \chi \equiv r_1 N_\varepsilon \le \varepsilon_1 N_\varepsilon$, $\varepsilon_1 = \varepsilon_1(\varphi, \vartheta_1)$.

In the next steps ($k = 1, 2, \ldots$) from differential equations (A10), (A11) we obtain the value corrections of the synovial fluid velocity components $v_{\varphi 1}$, $v_{\varphi 2}$, ..., $v_{\vartheta 1}$, $v_{\vartheta 2}$, ... caused by the unsteady conditions

and viscoelastic non-Newtonian properties of the fluid flowing in impulsive motion in circumference and meridian directions.

Now, we put the obtained components (A15) into the continuity equations [18], [22]. Hence we have:

$$\frac{\partial v_{\varphi 0}}{\partial \varphi}+\sin(\vartheta/R)\frac{\partial v_{r0}}{\partial r_1}+\frac{\partial}{\partial \vartheta_1}[v_{\vartheta 0}\sin(\vartheta/R)]=0,$$

$$\frac{\partial v_{\varphi 1}}{\partial \varphi}+\sin(\vartheta/R)\frac{\partial v_{r1}}{\partial r_1}+\frac{\partial}{\partial \vartheta_1}[v_{\vartheta 1}\sin(\vartheta/R)]=0,$$

.....

$$\frac{\partial v_{\varphi k}}{\partial \varphi}+\sin(\vartheta/R)\frac{\partial v_{rk}}{\partial r_1}+\frac{\partial}{\partial \vartheta_1}[v_{\vartheta k}\sin(\vartheta/R)]=0,$$

..... (A19)

We integrate both sides of equations $(A19)_0$ with respect to the variable r_1. Hence we obtain velocity component in radial direction and its corrections in the following form:

$$v_{r0}(v_{\varphi 0}, v_{\vartheta 0}),\quad v_{r1}(v_{\varphi 1}, v_{\vartheta 1}), ..., v_{rk}(v_{\varphi k}, v_{\vartheta k}), ... \tag{A20}$$

The synovial fluid velocity component v_{r0} in the gap-height direction equals zero in bone head surface. Therefore, after imposing the boundary condition $v_{r0} = 0$ for $r_1 = 0$, on equation (A19), the synovial fluid velocity component in the gap-height direction has the following form [22]:

$$v_{r0}(\varphi, r_1, \vartheta_1, t_1)=-\frac{N_\varepsilon e^{-\varepsilon_{T1}^2 N_\varepsilon^2}}{erf(\varepsilon_{T1}N_\varepsilon)}$$

$$\times\left[\frac{\partial \varepsilon_{T1}}{\partial \varphi}-\frac{\sqrt{\pi}}{2}\left(\frac{1}{\sin^2\vartheta_1}\frac{\partial \varepsilon_{T1}}{\partial \varphi}\frac{\partial p_{10}}{\partial \varphi}+\frac{\partial \varepsilon_{T1}}{\partial \vartheta_1}\frac{\partial p_{10}}{\partial \vartheta_1}\right)\right.$$

$$\left.\times\frac{1}{N_\varepsilon}\int_0^{\varepsilon_{T1}N_\varepsilon} e^{\chi_1^2} erf\chi_1 d\chi_1\right]\int_0^{r_1}\frac{erf(r_2N_\varepsilon)}{erf(\varepsilon_{T1}N_\varepsilon)}dr_2$$

$$-\frac{\sqrt{\pi}}{2}\left(\frac{1}{\sin^2\vartheta_1}\frac{\partial^2 p_{10}}{\partial \varphi^2}+\frac{\partial^2 p_{10}}{\partial \vartheta_1^2}+\frac{\partial p_{10}}{\partial \vartheta_1}\cot\vartheta_1\right)$$

$$\times\left\{\frac{1}{N_\varepsilon^2}Y_0(\chi=\varepsilon_{T1}N_\varepsilon)\int_0^{r_1}\frac{erf(r_1N_\varepsilon)}{erf(\varepsilon_{T1}N_\varepsilon)}dr_1\right.$$

$$\left.-\int_0^{r_1}Y_0(\chi_1=r_2N_\varepsilon)\,dr_2\right\}, \tag{A21}$$

where: $0 \le t_1 < \infty$, $0 \le r_2 \le r_1 \le \varepsilon_{T1}$, $\pi/8 \le \vartheta_1 \le \pi/2$, $0 < \varphi < 2\pi\theta_1$, $0 \le \theta_1 < 1$, $0 \le \chi_2 \le \chi_1 \le \chi \equiv r_1N_\varepsilon \le \varepsilon_{T1}N_\varepsilon \equiv M_\varepsilon$.

The synovial fluid velocity component v_{r0} in the gap-height direction presented in (A21) does not equal zero on acetabulum surface. Similarly obtained functions of velocity corrections v_{r1}, v_{r2}, ... equal zero on acetabulum surface. Therefore, integrating the continuity equation $(A19)_1$, $(A19)_2$, ... with respect to the variable r_1 and imposing the boundary condition $(A14)_3$ for $r_1 = \varepsilon_1$ on the velocity component in the gap-height direction, and taking into account the conditions $(A13)_3$ for $r_1 = 0$, we obtain the following equations:

$$\frac{1}{\sin\vartheta_1}\frac{\partial}{\partial \varphi}\int_0^{\varepsilon_{T1}} v_{\varphi 0}(p_{10})dr_1+\frac{1}{\sin\vartheta_1}\frac{\partial}{\partial \vartheta_1}$$

$$\int_0^{\varepsilon_{T1}} v_{\vartheta 0}(p_{10})\sin\vartheta_1 dr_1=-Str\frac{\partial \varepsilon_{T1}}{\partial t_1}, \tag{A22}$$

$$\frac{1}{\sin\vartheta_1}\frac{\partial}{\partial \varphi}\int_0^{\varepsilon_{T1}} v_{\varphi 1}(p_{11})dr_1$$

$$+\frac{1}{\sin\vartheta_1}\frac{\partial}{\partial \vartheta_1}\int_0^{\varepsilon_{T1}} v_{\vartheta 1}(p_{11})\sin\vartheta_1 dr_1=0, \tag{A22}$$

$$\frac{1}{\sin\vartheta_1}\frac{\partial}{\partial \varphi}\int_0^{\varepsilon_{T1}} v_{\varphi 2}(p_{12})dr_1$$

$$+\frac{1}{\sin\vartheta_1}\frac{\partial}{\partial \vartheta_1}\int_0^{\varepsilon_{T1}} v_{\vartheta 2}(p_{12})\sin\vartheta_1 dr_1=0, \tag{A22}$$

.....

$$\frac{1}{\sin\vartheta_1}\frac{\partial}{\partial \varphi}\int_0^{\varepsilon_{T1}} v_{\varphi k}(p_{1k})dr_1$$

$$+\frac{1}{\sin\vartheta_1}\frac{\partial}{\partial \vartheta_1}\int_0^{\varepsilon_{T1}} v_{\vartheta k}(p_{1k})\sin\vartheta_1 dr_1=0, \tag{A22}$$

.....

Putting functions $v_{\varphi 0}$, v_{r0}, i.e., (A16), (A17) into $(A21)_0$ we obtain equation (14), which determines unknown pressure p_{10}. Putting functions $v_{\varphi 1}$, v_{r1}; $v_{\varphi 2}$, v_{r2}; ..., $v_{\varphi k}$, v_{rk}, ... into $(A21)_1$, $(A21)_2$, ..., $(A21)_k$, … we obtain equations which determine unknown pressure corrections: p_{11}, p_{12}, ..., p_{1k}, ..., respectively.

A3. Limits of coefficients for infinity time

If t_1 tends to infinity, i.e., N_ε tends to zero, then equation (18) tends to the classical known Reynolds equation for steady motion. To explain this fact we calculate the following limit [22]:

$$\lim_{N_\varepsilon\to 0}\frac{\sqrt{\pi}}{2N_\varepsilon^2}Y_0(\chi=\varepsilon_1 N_\varepsilon)\equiv\lim_{N_\varepsilon\to 0}\frac{\sqrt{\pi}}{2N_\varepsilon^2}$$

$$\times\left[\int_0^{\varepsilon_1 N_\varepsilon}\exp(\chi^2)erf(\chi)d\chi-erf(\varepsilon_1 N_\varepsilon)\int_0^{\varepsilon_1 N_\varepsilon}\exp(\chi^2)d\chi\right]$$

$$=\lim_{N_\varepsilon\to 0}\frac{1}{N_\varepsilon^2}\left\{\int_0^{\varepsilon_1 N_\varepsilon}\left[\exp(\chi_v^2)\int_0^{\chi}\exp(-\chi_{v1}^2)d\chi_{v1}\right]d\chi_v\right.$$

$$\left.-\left(\int_0^{\varepsilon_1 N_\varepsilon}\exp(-\chi_v^2)d\chi_v\right)\left(\int_0^{\varepsilon_1 N_\varepsilon}\exp(\chi_v^2)d\chi_v\right)\right\}$$

$$\overset{H}{=}-\lim_{N_\varepsilon\to 0}\frac{\varepsilon_1\int_0^{N_\varepsilon\varepsilon_1}\exp(\chi^2)d\chi_1}{2N_\varepsilon\exp(\varepsilon_1^2N_\varepsilon^2)}\overset{H}{=}$$

$$-\frac{\varepsilon_1^2}{2}\lim_{N_\varepsilon\to 0}\frac{\exp(\varepsilon_1^2N_\varepsilon^2)}{\exp(\varepsilon_1^2N_\varepsilon^2)+2\varepsilon_1^2N_\varepsilon^2\exp(\varepsilon_1^2N_\varepsilon^2)}=-\frac{\varepsilon_1^2}{2}. \tag{A23}$$

Analogously:

$$\lim_{N_\varepsilon\to 0}\frac{\sqrt{\pi}}{2N_\varepsilon^2}Y_0(\chi_1=N_\varepsilon r_1)=-\frac{r_1^2}{2}, \tag{A24}$$

$$\lim_{N_\varepsilon\to 0}\frac{erf(r_1N_\varepsilon)}{erf(\varepsilon_1N_\varepsilon)}=\frac{r_1}{\varepsilon_1}. \tag{A25}$$

We calculate the following limits:

$$\lim_{N_\varepsilon\to 0}W_{ef}^*(\varepsilon_{T1s}N_\varepsilon)\equiv\lim_{N_\varepsilon\to 0}\frac{N_\varepsilon\exp(-N_\varepsilon^2\varepsilon_{T1s}^2)}{\int_0^{\varepsilon_{T1s}}e^{-\chi_1^2}d\chi_1}$$

$$=\lim_{N_\varepsilon\to 0}\frac{\exp(-N_\varepsilon^2\varepsilon_{T1s}^2)-2N_\varepsilon^2\varepsilon_{T1s}^2\exp(-N_\varepsilon^2\varepsilon_{T1s}^2)}{\varepsilon_{T1}\exp(-N_\varepsilon^2\varepsilon_{T1s}^2)}=\frac{1}{\varepsilon_{T1s}}, \tag{A26}$$

and

$$\lim_{N_\varepsilon\to 0}\left(\frac{\partial^2W_{ef}(\varepsilon_{T1}N_\varepsilon)}{\partial\delta_1^2}\right)_{\delta_1=0}=-\lim_{N_\varepsilon\to 0}W_{ef}^*(\varepsilon_{T1s}N_\varepsilon)$$

$$+2\lim_{N_\varepsilon\to 0}[N_\varepsilon^2\varepsilon_{T1s}+W_{ef}^*(\varepsilon_{T1s}N_\varepsilon)]W_{ef}^*(\varepsilon_{T1s}N_\varepsilon)W_{ef}(\varepsilon_{T1s}N_\varepsilon)$$

$$=-\frac{1}{\varepsilon_{T1s}}+2\left(0+\frac{1}{\varepsilon_{T1s}}\right)\frac{1}{\varepsilon_{T1s}}\frac{\varepsilon_{T1s}}{2}=0, \tag{A27}$$

and

$$\lim_{N_\varepsilon\to 0}\left(\frac{\partial W_{ef}(\varepsilon_{T1}N_\varepsilon)}{\partial\delta_1}\right)_{\delta_1=0}$$

$$=1-\lim_{N_\varepsilon\to 0}W_{ef}^*(\varepsilon_{T1s}N_\varepsilon)\lim_{N_\varepsilon\to 0}W_{ef}(\varepsilon_{T1s}N_\varepsilon)$$

$$=1-\frac{1}{\varepsilon_{T1s}}\frac{\varepsilon_{T1s}}{2}=\frac{1}{2}, \tag{A28}$$

$$2\lim_{N_\varepsilon\to 0}\frac{\sqrt{\pi}}{2N_\varepsilon^2}\left(\frac{\partial Y_0(\varepsilon_{T1}N_\varepsilon)}{\partial\delta_1}\right)_{\delta_1=0}$$

$$=\lim_{N_\varepsilon\to 0}2\frac{\sqrt{\pi}}{2N_\varepsilon^2}\left(\frac{-2N_\varepsilon}{\sqrt{\pi}}\right)e^{-N_\varepsilon^2\varepsilon_{T1s}^2}\int_0^{\varepsilon_{T1s}N_\varepsilon}e^{\chi_1^2}d\chi_1$$

$$=-2\lim_{N_\varepsilon\to 0}\left(-2N_\varepsilon\varepsilon_{T1s}^2\int_0^{\varepsilon_{T1s}N_\varepsilon}e^{\chi_1^2}d\chi_1+\varepsilon_{T1s}\right)=-2\varepsilon_{T1s}, \tag{A29}$$

thus

$$\lim_{N_\varepsilon\to 0}\frac{\sqrt{\pi}}{2N_\varepsilon^2}\left(\frac{\partial^2Y_0(\varepsilon_{T1}N_\varepsilon)}{\partial\delta_1^2}\right)_{\delta_1=0}$$

$$=-1+2\lim_{N_\varepsilon\to 0}N_\varepsilon\varepsilon_{T1s}e^{-N_\varepsilon^2\varepsilon_{T1s}^2}\int_0^{\varepsilon_{T1s}N_\varepsilon}e^{\chi_1^2}d\chi_1=-1, \tag{A30}$$

hence:

$$\frac{\sigma_{s1}^2}{2!}\lim_{N\to 0}\frac{\sqrt{\pi}}{2N_\varepsilon^2}\left(\frac{\partial^2J(\varepsilon_{T1}N_\varepsilon)}{\partial\delta_1^2}\right)_{\delta_1=0}$$

$$=\frac{\sigma_{s1}^2}{2!}\left[-\frac{\varepsilon_{T1s}^2}{2}\times 0-2\varepsilon_{T1s}\times\frac{1}{2}+\frac{\varepsilon_{T1s}}{2}\times(-1)-(-\varepsilon_{T1s})\right]$$

$$=-\frac{\sigma_{s1}^2}{4}\varepsilon_{T1s}.$$

A4. Application of unified calculation algorithm

Modified stochastic Reynolds equations (14), (17), (20), (30) are brought to the following partial, second order non homogeneous recurrence equation [18] with variable coefficients $S(i, j)$, $Z(i, j)$ and free term $Q(i, j)$:

$$S_{\kappa}(i,j)\, p_{i+1,j} + S_{\nu}(i,j)\, p_{i,j+1} + S_{\pi}(i,j)\, p_{i,j-1} + S_{\xi}(i,j)\, p_{i-1,j} - Z(i,j)\, p_{i,j} = Q(i,j)\,. \quad \text{(A31)}$$

Numerical calculations are performed in spherical coordinates inside region $\Omega(\alpha_1, \alpha_3)$ for $\alpha_1 = \varphi$, $\alpha_3 = \vartheta_1$, where:

$$\Omega(\varphi_i, \vartheta_{1j}) : \begin{cases} i = 1, 2, 3, ..., M \\ j = 1, 2, 3, ..., N. \end{cases} \quad \text{(A32)}$$

Spherical region Ω contains NM calculation nods, where $N = M = 100$ steps located on the spherical cap presented in figure A1:

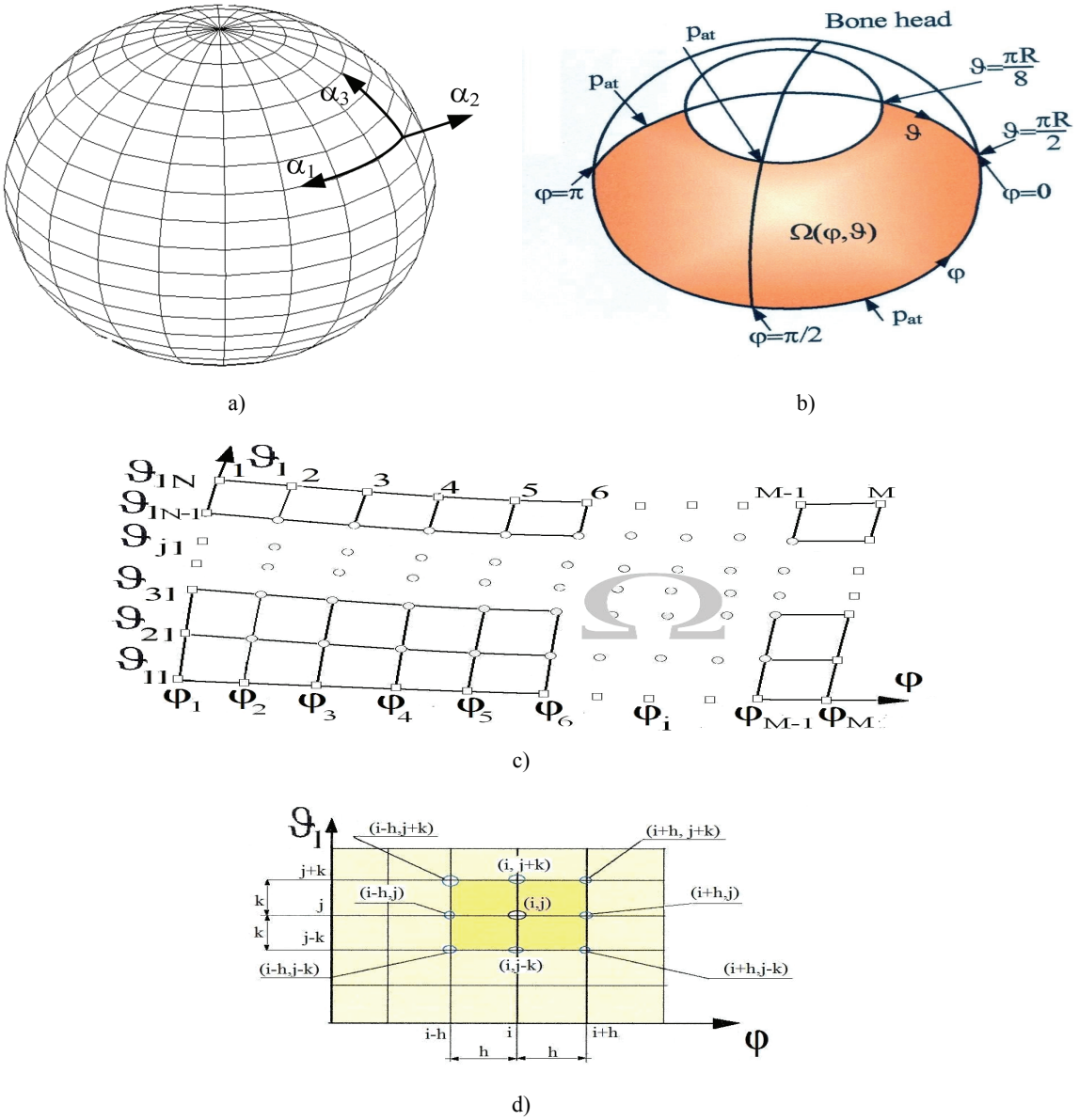

Fig. A1. Spherical surfaces and regions: (a) sphere, (b) region Ω on the sphere as a spherical cap, (c) expansion of region Ω, (d) individual calculation nod